The *Drosophila* AWP1 ortholog Doctor No regulates JAK/STAT signaling for left-right asymmetry in the gut by promoting Domeless receptor endocytosis

(AWP1 のショウジョウバエ・オーソログである Doctor No は Domeless 受容体のエンドサイトーシスを促進することで腸の左右非対称性形成において JAK/STAT シグナルを制御する)

A Thesis

Submitted to the
Department of Biological Sciences, Graduate School of Science,
Osaka University
in partial fulfillment of
the requirements for the degree of Doctor of Philosophy

by
Yi-Ting Lai

Supervisor: Dr. Kenji Matsuno

Committee member: Dr. Hiroki Nishida

Committee member: Dr. Hiroki Oda

SUMMARY

The molecular mechanisms of left-right (LR) asymmetric development are a principal question in developmental biology. In invertebrates, the mechanisms to establish their LR asymmetry are not as conserved as the well-known systems including nodal flow in vertebrates. Many internal *Drosophila* organs show stereotypical LR asymmetry, for which the underlying mechanisms remain elusive. Through genetic screens, an evolutionarily conserved ubiquitin-binding protein, AWP1/Doctor no (Drn) was identified as a novel factor required for the LR asymmetry of the embryonic anterior gut in *Drosophila*. In this study, the results showed that *drn* is essential in the circular visceral muscle cells of the midgut for JAK/STAT signaling, which contributes to the first known cue for anterior gut lateralization via LR-asymmetric nuclear rearrangement. Mutants of various JAK/STAT signaling components also showed LR laterality defects in the embryonic anterior gut. Taken together, these results suggest a role of JAK/STAT signaling in regulating LR-asymmetric development. To confirm whether *drn* interacts with JAK/STAT signaling in other contexts during development, characteristic phenotypes associated with JAK/STAT signaling were examined. Embryos homozygous for *drn* and lacking its maternal contribution showed phenotypes similar to that of depleted JAK/STAT signaling, such as disturbed expression of a pair-rule gene, *even-skipped* (*eve*), and truncation of the trachea in the embryos, suggesting that Drn acts as a general component that positively regulates JAK/STAT signaling.

Since the mammalian ortholog AWP1 binds ubiquitin and modulates functions of ubiquitinated proteins, I hypothesized that Drn might be involved in regulating endocytic trafficking of the JAK/STAT signaling pathway in *Drosophila*. To test this hypothesis, the

colocalization of Drn with various endosomal compartments was examined. Drn appeared to localize to endocytic compartment markers such as Hrs, Rab5, Rab7, and LAMP1 at low frequency, which is consistent with the idea that Drn plays a role in endocytic trafficking. Furthermore, loss of Drn resulted in the specific accumulation of Domeless (Dome), the receptor for JAK/STAT signaling, in intracellular compartments including ubiquitinated cargos. Immunohistochemical data also showed that Dome colocalized with Drn in wild-type embryos. These results suggest that Drn is required for the endocytosis of Dome, which is a critical step in the activation of JAK/STAT signaling and subsequent degradation of Dome, as shown in previous studies. Overall, this study presents a working model of *drn*, a novel gene required for the strict regulation of JAK/STAT signaling through controlling endocytosis of Dome receptor, which is a mechanism involved in LR-asymmetric morphogenesis in the *Drosophila* anterior gut.

Table of Contents

INTRODUCTION

The animal body plan is elaborately programmed by various signaling molecules during development. The molecular mechanisms regulating development are the fundamental questions that developmental biologists are keen to solve since centuries ago. To date, many developmental processes and gene regulatory networks have been revealed, but still more remain under-discovered. The early development of bilaterians is initiated by the establishment of three different body axes, anterior-posterior (AP), dorsal-ventral (DV), and left-right (LR), which define the spatial cues for cells to proliferate and differentiate (Arendt and Nübler-Jung, 1997; Kimelman and Martin, 2012; Levin, 2005). Fascinating but also counterintuitive, while most bilaterians appear externally LR-symmetric, nearly all have LR-asymmetric internal structures. The question: "Why does left-right patterning exist?" has been perplexing developmental biologists since long ago. To answer this question, it is crucial to understand the thorough mechanisms of how LR asymmetry is developed in bilateral animals (Levin, 2005). It is known that most of the LR-asymmetric structures are strongly biased to one side of the LR axis, such as the coiling of the snail shell and the internal organs in vertebrates (Blum and Ott, 2018). Such LR asymmetry is referred to as "directional LR asymmetry". What seem more intriguing are the evolutionarily diverse mechanisms of LR laterality establishment between different species (Blum and Ott, 2018; Levin, 2005; Namigai et al., 2014). For example, the well-studied development of LR asymmetry in vertebrates is known to be patterned by the core components of the LR axis, *Nodal*, *Lefty1/2*, and *Pitx2*, which are initiated by the flow of embryonic fluid induced by directional cilial rotation in some species (Yoshiba and Hamada, 2014). However, *Nodal* does not exist in

ecdysozoans such as insects and nematodes, and different mechanisms have been indicated for patterning LR in these species (Blum and Ott, 2018). In invertebrates, some studies have been done to reveal the importance of actomyosin in driving cellular chirality, which subsequently induces LR-asymmetric development in *D. melanogaster* and *C. elegans* (Baum, 2006; Naganathan et al., 2016). However, the comprehensive mechanisms underlying LR-asymmetric development in invertebrates remain largely unknown, which has drawn much attention from researchers (Vandenberg and Levin, 2013).

Stereotypical LR asymmetry is present in several organs of *Drosophila*, including the gut, testis, male genitalia, and brain (Coutelis et al., 2014; Okumura et al., 2008).Of these organs, the embryonic gut is the first to show LR asymmetry during development (Hayashi and Murakami, 2001; Hozumi et al., 2006). Intriguingly, the anterior and posterior parts of the embryonic gut are controlled by two distinct gene groups. The LR asymmetry of the posterior part is regulated by *Myo1D*, which determines cell chirality (Hozumi et al., 2006; Inaki et al., 2016; Inaki et al., 2018; Nakamura et al., 2013; Spéder et al., 2006; Utsunomiya et al., 2019). An entirely different mechanism governs the LR asymmetry of the anterior part. The anterior gut of the embryo consists of the foregut (FG) and midgut (MG), which are complex structures with directional and stereotypical LR asymmetry (Fig. 1A, B) (Hayashi and Murakami, 2001). Various genetic pathways, including the JNK and Wnt pathways, play important roles in LR-asymmetric development (Hayashi et al., 2005; Kuroda et al., 2012; Maeda et al., 2007; Okumura et al., 2010; Shin et al., 2021; Taniguchi et al., 2007). A genetic screen performed by our group suggested that the Janus kinase (JAK)-signal transducer and activator of transcription (STAT) signaling pathway is also involved in LR-asymmetric

development. The present study revealed the involvement of JAK/STAT signaling in LR-asymmetric development of the anterior gut.

JAK/STAT signaling, which is evolutionarily conserved from *Drosophila* to humans, is essential for morphogenesis, cell proliferation, cell differentiation, cell death, immunity, and other biological events (Arbouzova and Zeidler, 2006; Calò et al., 2003; Lee et al., 2017; Myllymäki and Rämet, 2014; Recasens-Alvarez et al., 2017; Seif et al., 2017). In JAK/STAT signaling in *Drosophila*, the ligands are encoded by *unpaired* (*upd*), *upd-2*, and *upd-3* and the receptor is encoded by *domeless* (*dome*) (Agaisse et al., 2003; Brown et al., 2001; Ghiglione et al., 2002; Harrison et al., 1998; Hombría et al., 2005). JAK is encoded by *hopscotch* (*hop*) in *Drosophila*. Moreover, similar to the mammalian JAK/STAT system, Hop constitutively associates with the intracellular domain of Dome in *Drosophila* (Arbouzova and Zeidler, 2006; Binari and Perrimon, 1994). Ligand binding induces conformational changes in Dome that lead to the phosphorylation of JAK, which phosphorylates Dome to create docking sites for STATs, particularly Stat92E in *Drosophila* (Yan et al., 1996). JAK then tyrosine phosphorylates STATs, which are subsequently dimerized and translocated to the nucleus to bind to enhancers of target genes and activate transcription (Arbouzova and Zeidler, 2006; Hou et al., 1996; Yan et al., 1996) (diagram provided in Fig. 5A).

In mammals, endocytosis regulates JAK/STAT signaling through various mechanisms (German et al., 2011; Lei et al., 2011). Endocytosis and the regulation of JAK/STAT signaling activity are also closely connected in *Drosophila* (Devergne et al., 2007; Moore et al., 2020; Ren et al., 2015; Vidal et al., 2010). In the classic working model

of endocytosis, membrane receptors are internalized into endosomal compartments, where they are degraded and recycled. This reduces the number of receptors available to transduce signaling (Cendrowski et al., 2016; Elkin et al., 2016; Piper et al., 2014). Moreover, receptor activity requires endocytic trafficking in some signaling pathways (Cendrowski et al., 2016; Irannejad et al., 2013). Studies on the relationship between endocytosis and JAK/STAT signaling in *Drosophila* have provided contradictory results regarding whether endocytosis upregulates or downregulates JAK/STAT activity (Devergne et al., 2007; Moore et al., 2020; Ren et al., 2015; Vidal et al., 2010). To clarify these conflicting results, it would be helpful to identify and examine a factor that specifically regulates the endocytosis of Dome.

In this study, I found that the *Drosophila* ortholog of AWP1 (associated with PRK1, also known as ZFAND6), referred to as Dr. No (Drn), positively regulates JAK/STAT signaling by facilitating the endocytic trafficking of the Dome receptor, which is required for normal LR-asymmetric development of the embryonic gut. *Drosophila* Drn was named after Ian Fleming's fictional character, whose heart was located on the right side of his chest (Fleming, 1958). Drn protein contains an A20-type zinc finger at the N-terminus and an AN1-type zinc finger at the C-terminus; this is similar to the mammalian ortholog, which was first identified in humans and mice (Duan et al., 2000). In vertebrates, AWP1 proteins bind to ubiquitin, regulate NF-κB activity, and stimulate the export of Pex5 from the peroxisome, among other roles (Chang et al., 2011; Fenner et al., 2009; Miyata et al., 2012). During *Xenopus* development, AWP1 modifies Wnt and FGF signaling to specify neural crest cells (Seo et al., 2013). However, the molecular mechanisms by which AWP1/Drn proteins influence these various cell signaling pathways are not well understood. In this study, I found

that AWP1/Drn plays a crucial role in internalizing the Dome receptor and proposed a novel mechanism by which AWP1/Drn positively modulates JAK/STAT signaling.

RESULTS

Part 1 - *drn* is involved in LR-asymmetric development of the embryonic anterior gut through JAK/STAT pathway

drn mutations affect LR-asymmetric gut morphogenesis in *Drosophila*

To identify genes that affect LR asymmetry in the anterior gut, including the FG and anterior midgut (AMG), a genetic screen using a large collection of P element insertion lines (*Drosophila* Genes Search Project, http://kyotofly.kit.jp/stocks/documents/_GS_lines.html) (Toba et al., 1998) was conducted by previous members in the Matsuno laboratory. LR asymmetry phenotypes of the FG and AMG were scored for mutants obtained from the genetic screen. The FG is composed of the pharynx, esophagus (ES), and proventriculus (PV), which is a valve-like structure connecting the FG to the AMG (Fig. 1A, B). The definitions of normal LR asymmetry in the FG and AMG are as follows: (1) When viewed from the ventral side, the wild-type *Drosophila* ES loops in an inverse C shape and is connected to the PV (100%, N = 50); this was defined as normal FG laterality (Fig. 1A). (2) The joint between the PV and AMG is located on the right side of the midline in wild-type embryos (100%, N = 50); this was defined as normal laterality of the AMG (Fig. 1A). Using these criteria, a previous graduate student, Reo Maeda, identified two mutant lines, GS12294 and GS10567, which affect LR asymmetry in the FG and AMG (Fig. 1C).

These lines carry a P element insertion in the *CG45050* locus (Fig. 1D). In this study, the *CG45050* gene was named as *drn*. *Drosophila* Drn and human AWP1 share 42.1%

identity and 62.2% similarity in terms of the whole protein (calculated using EMBOSS Pairwise Alignment Algorithms) (Fig. 1E). In particular, an A20-type zinc finger (amino acids 6–40) and an AN1-type zinc finger (amino acids 137–180) are highly conserved (Fig. 1E). A20-type zinc fingers are found in various proteins with ubiquitin-editing functions; these proteins are often associated with human pathogenesis (Heyninck and Beyaert, 1999; Jacque and Ley, 2009; Kim et al., 2021; Rothe et al., 1995; Song et al., 1996). LR asymmetry defects of the anterior gut were found in 42.5% of *Drosophila* embryos homozygous for $drn^{GS12294}$ and 13.0% of those homozygous for $drn^{GS10567}$, indicating a disturbance in LR-asymmetrical development (Fig. 1C, F). In contrast, hindgut and posterior MG laterality were normal in all cases examined (N = 40), indicating heterotaxy but not situs inversus in these phenotypes. To genetically characterize *drn* gene further, deletion mutant alleles of *drn* were generated by imprecise P element excision. In drn^{1}, the deduced initiation codon and 5′ portion of the coding region were deleted from the *drn* alternative RNA products CG45050-RB, -RC, -RD, -RE, -RF, and -RG (Fig. 1D). In drn^{2}, the deduced initiation codon and most coding sequences were deleted from all *drn* alternative RNA products, suggesting that drn^{2} is a loss-of-function mutant of *drn* (Fig. 1D). Various degrees of LR asymmetry defects were observed in drn^{1} or drn^{2} homozygotes and transheterozygotes, demonstrating that mutations in *drn* are responsible for the LR defect phenotypes (Fig. 1F, G). These mutant embryos had LR defects in both the FG and AMG or in the AMG alone (orientation of the FG was correct, but the joint between the FG and PV was on the opposite side); however, they never had defects in the FG alone (Fig. 1F, G). Thus, LR asymmetry defects in the FG are strictly coupled with those in the AMG, suggesting the primary role of the AMG in LR-asymmetric

development of the anterior gut, as has been observed in other mutants with defective LR asymmetry (Kuroda et al., 2012; Taniguchi et al., 2007). I also noted relatively mild LR defects in heterozygotes of *drn*^{1} or *drn*^{2}, indicating that *drn* may behave in a semidominant manner (Fig. 1F).

drn is required for the LR-asymmetric rearrangement of circular visceral muscle (CVMU) cells

To confirm whether *drn* is required for LR-asymmetric development of the anterior gut, rescue experiments were performed using the GAL4/UAS system (Brand and Perrimon, 1993). The expression of wild-type *drn* encoded by *UAS-drn* is driven by various tissue-specific GAL4 drivers in a *drn*^{1} homozygote mutant background (Brand and Perrimon, 1993; Elliott and Brand, 2008). The FG and AMG are composed of the epithelium, CVMU, and longitudinal visceral muscle (LVMU) (Fig. 2A). LR defects of the FG and AMG in *drn*^{1} homozygotes were reduced by half when *UAS-drn* was introduced without any GAL4 driver (negative control), probably due to the leaky expression of *UAS-drn* (Fig. 1F, 2B). On the other hand, these LR defects were efficiently rescued by *UAS-drn* misexpression driven by *da*-GAL4 (ubiquitous), *NP1522* (in the somatic muscle and CVMU), *hand*-GAL4 (in the CVMU), *24B*-GAL4 (in the CVMU, LVMU, and somatic muscle), and *48Y*-GAL4 (in the AMG epithelium, CVMU, and LVMU) (Fig. 2B). In contrast, LR defects were not rescued by *UAS-drn* misexpression driven by *NP0221* (in the LVMU), *NP5021* (in the epithelium), or *elav-GAL4* (in the nervous system) (Fig. 2B). Collectively, the data suggest that *drn* expression is primarily required in the CVMU but not in the LVMU or other tissues for

normal LR-asymmetric development of the FG and AMG. I that in wild-type embryos, *UAS-drn* misexpression driven by the GAL4 drivers tested here did not induce marked LR defects in the FG and AMG, suggesting that enhanced *drn* expression did not affect LR-asymmetric development in wild-type embryos (Fig. 2C).

Previous analyses by our group revealed that the LR asymmetric tilt of the ellipsoidal nuclei in the CVMU cells covering the MG epithelium is the first disruption of LR symmetry in the anterior gut (Fig. 3A) (Kuroda et al., 2012; Okumura et al., 2010; Shin et al., 2021; Taniguchi et al., 2007). At early stage 15, the major axis of the ellipsoidal nuclei in the CVMU cells was still perpendicular to the midline of the AMG (Fig. 3A). When the MG chambers began dividing at late stage 15, the nuclei in the lower 30% of the presumptive first chamber on the right began tilting diagonally upward and to the right (Fig. 3A). This LR-asymmetric nuclear tilt preceded the LR-asymmetric morphological changes in the AMG, indicating that it was not a consequence of LR-asymmetric morphogenesis (Taniguchi et al., 2007). To analyze whether this process was disrupted in *drn* mutants, *65E04-GAL4* was used to specifically express nuclear-localizing RedStinger fluorescent proteins in the visceral muscles. The angle (θ) between the major axis of the ellipsoidal nuclei in the lower 30% of the presumptive first chamber and the anterior–posterior axis of the embryo was measured by a double-blind test at late stage 15 (Fig. 3B). Consistent with previous results published by our lab, the angle measured was smaller for nuclei on the right side than for those on the left side in wild-type embryos ($P < 0.0001$, K–S test) (Fig. 3C, C') (Kuroda et al., 2012; Okumura et al., 2010; Taniguchi et al., 2007). However, in drn^{1} homozygotes, no significant difference was noted in the angle between the left and right sides. Moreover, the angle

remained closer to perpendicular on both sides even at late stage 15 (P = 0.765, K–S test) (Fig. 3D, D'). In addition to the LR-asymmetric tilting of the nuclei, a paper published by our lab previously reported that the nuclei assemble in belt-shaped zones along the anterior–posterior axis. These nuclei are scattered in mutants with defects in LR asymmetry of the anterior gut (Shin et al., 2021). In this study, I observed that the distribution of nuclei was more dispersed in *drn*^{1} homozygotes than in wild-type embryos in all cases examined (N = 10) (Fig. 3C, D). Collectively, these results suggest that *drn* contributes to LR-asymmetric development of the AMG by regulating the LR-asymmetric rearrangement of nuclei in CVMU cells.

To verify the roles of *drn* in the CVMU, I assessed the distribution of *drn* mRNA in embryos by *in situ* hybridization at various stages of embryogenesis (Fig. 4A–D). Comprehensive analyses of gene expression in *Drosophila* revealed that *drn* is highly expressed in early embryonic stages (Thurmond et al., 2019). *drn* mRNA was strongly detected in the preblastoderm to blastoderm (stage 5) stages, suggesting that *drn* mRNA is maternally provided (Fig. 4A, B). I also found that *drn* was broadly expressed at stages 11 and 15, including the trunk visceral mesoderm (TVM, the primordium of the CVMU), wherein *drn* was required for LR-asymmetric development of the anterior gut (Fig. 4C). In contrast, the negative control (sense probe) exhibited no signal under the same conditions (Fig. 4E–H).

JAK/STAT signaling is involved in the LR-asymmetric development of the anterior gut

Although previous research has suggested that Drn negatively regulates JAK/STAT signaling in cultured *Drosophila* cells (Vidal et al., 2010), the role of Drn was not further explored *in vivo*. As *drn* is involved in JAK/STAT signaling, we hypothesized that JAK/STAT signaling plays a role in LR-asymmetric morphogenesis of the anterior gut. Various mutants of genes involved in the JAK/STAT signaling pathway, including *dome*, *Stat92E*, *upd*, and *hop*, were scored for LR phenotypes (Fig. 5B). The roles of these gene products are schematically presented in Fig. 5A. These mutants showed various degrees of LR defects in the FG and AMG, indicating that JAK/STAT signaling is indispensable for normal LR-asymmetric development of the anterior gut (Fig. 5B). In addition, when JAK/STAT signaling was augmented by misexpression of an activated form of Hop (*UAS-hop*$^{Tum\text{-}l}$) (Harrison et al., 1995), specifically in CVMU cells under the control of *hand-GAL4* or *24B-GAL4*, the embryos showed LR defects in the FG and AMG (Fig. 5B). Therefore, excessive activation of JAK/STAT signaling can also disrupt the LR asymmetry of the FG and AMG. Taken together, these findings indicate that JAK/STAT signaling activity must be maintained at proper levels for LR-asymmetric development of the anterior gut.

drn is a general component of the JAK/STAT signaling pathway

To analyze the connection between *drn* and JAK/STAT signaling more directly, I assessed the characteristic phenotypes relating to JAK/STAT signaling in *drn* mutants.

The expression of a pair-rule gene, *even-skipped* (*eve*), was disturbed in embryos homozygous for *Stat92E*, such as *Stat92E*^{HJ}, with approximately 67% of the embryos showing aberrant phenotypes, such as weak stripe 3 (19%), fusion between stripes 2 and 3

(19%), or fusion between stripes 5 and 6 (67%) (N = 27), rather than the seven-stripe pattern noted in wild-type embryos (Fig. 5C–D') (Yan et al., 1996). The *eve* expression in embryos homozygous for drn^{2} was analyzed, and I found that all embryos had normal *eve* expression and displayed a normal seven-stripe pattern (N = 20) (Fig. 5E). As I found that the mRNA of *drn* is maternally supplied (Fig. 4A, B), maternal *drn* was genetically removed from drn^{2} homozygotes ($drn^{2\ m/z}$). The phenotypes of $drn^{2\ m/z}$ embryos were similar to those of $Stat92E^{HJ}$ homozygotes (36%, N = 33) (Fig. 5F, F'). These results suggest that *drn* is required for JAK/STAT signaling, with Stat92E playing an essential role. To further verify this idea, trachea morphology, which is controlled by JAK/STAT signaling in later embryonic stages (stages 15–17) (Li et al., 2003), was examined. The trachea was detected by CBP546 staining (Dong et al., 2014). In $Stat92E^{HJ}$ homozygotes, the dorsal trunk of the trachea was disturbed compared with that in wild-type embryos (Fig. 5G, H). Moreover, it was truncated in some drn^{2} homozygotes (35%, N = 20) and $drn^{2\ m/z}$ embryos (33%, N = 21). Defects in $drn^{2\ m/z}$ embryos were more severe than those in $drn^{2\ z}$ homozygotes, which can be predicted from the maternal contribution of *drn* (Fig. 5I, J). These results suggested that similar to *Stat92E*, *drn* plays a positive role in JAK/STAT signaling during embryonic development.

To further verify this possibility, I assessed whether the ubiquitous misexpression of *drn*, driven by *actin5c-GAL4*, could rescue LR defects in embryos homozygous for $Stat92E^{06346}$. The embryos homozygous for $Stat92E^{06346}$ showed LR defects in the anterior gut at a frequency of 25% (Fig. 5K); however, the ubiquitous misexpression of *drn* reduced the frequency of LR defects to 4% (Fig. 5K). This result can be explained by a previous finding that *Stat92E* exhibits a maternal effect (Hou et al., 1996; Li et al., 2003; Tsurumi et

al., 2011). I speculated that the supply of maternal *Stat92E* to *Stat92E*^{06346} mutant embryos is sufficient to support the activity of overexpressed *drn*, which can consequently rescue LR defects of these embryos.

Moreover, I examined whether upregulation of *drn* augments the activity of JAK/STAT signaling. JAK/STAT activity was assessed with the 10xSTAT-GFP reporter, a previously established GFP reporter responding to JAK/STAT signaling (Bach et al., 2007). 10xSTAT-GFP expressed on the trachea pits of each segment, resembling expression pattern of the JAK/STAT ligand, Upd (Bach et al., 2007). Effect of *drn* upregulation was examined with ubiquitously misexpression of *UAS-myc-drn* via *da-GAL4*. I noted that uniformed upregulation of *drn* did not noticeably alter the expression intensity or region of 10xSTAT-GFP (Fig. 6A–B'). The result is further confirmed with *in situ* hybridization of *trachealess* (*trh*) and *ventral vein lacking* (*vvl*), two known major target genes downstream of JAK/STAT signaling, expressed in the tracheal placodes during embryo development (Brown et al., 2001). mRNA expression of *trh* and *vvl* were found to be identical to wild-type expression (Fig. 6C–F), suggesting that upregulation of *drn* does not necessarily enhance JAK/STAT activity.

Additionally, I examined if the activity of JAK/STAT signaling showed LR-asymmetric activation in the anterior gut with the 10xSTAT-GFP reporter. However, such LR asymmetry activity was not identified, as 10xSTAT-GFP was expressed LR-symmetrically in wild-type embryos (Fig. 7).

In particular, these studies demonstrated that *drn* positively contributes to the activation of JAK/STAT signaling in three different developmental contexts. Therefore, I

proposed that Drn is a general component positively acting on JAK/STAT signaling, although a previous study involving knockdown by RNA interference (RNAi) and a reporter assay revealed that wild-type *drn* could downregulate JAK/STAT signaling in cultured *Drosophila* cells (Vidal et al., 2010). The cause of this discrepancy is unclear but may involve a negative feedback loop that is active in a particular time frame during JAK/STAT signaling, as detected by the reporter assay in cultured cells.

RESULTS

Part 2 - *drn* is required for the endocytosis of the Dome receptor to regulate JAK/STAT pathway

Drn partially localizes to various compartments of endocytic pathway

Although the biochemical roles of Drn have not been studied in *Drosophila*, the mammalian ortholog AWP1 binds to ubiquitin and modulates the functions of ubiquitinated proteins in mammals (Chang et al., 2011; Duan et al., 2000; Fenner et al., 2009). This process is often related to endocytic trafficking and the lysosomal breakdown of membrane receptors (Piper et al., 2014). Thus, I hypothesized that Drn is involved in endocytic trafficking that regulates the JAK/STAT signaling pathway. As TVM and CVMU cells are located deep inside the embryo, it is difficult to obtain clear microscopic images, making them unsuitable for analyzing the subcellular localization of Drn. However, *in situ* hybridization analysis revealed that *drn* is also expressed in the epidermis of the embryo (Fig. 4). Hence, I analyzed the potential colocalization of Drn with various endocytic compartments in the epidermis.

To detect Drn protein, a polyclonal antibody (anti-Drn antibody) against a full-length Drn was generated and its specificity was assessed by using the UAS-GAL4 system and RNAi against *drn* to deplete Drn in the stripe along the anterior-posterior boundary of the wing disc (the region expressing *ptc*). I found that the staining of anti-Drn antibody was largely absent from the stripe, confirming the specificity of the antibody (Fig. 8). Using this anti-Drn antibody, I examined the potential colocalization of Drn with various endosomal

compartments in the epidermis of wild-type embryos. Drn was detected as punctae in the cytosol and was occasionally found colocalized with endosomal markers, such as Hrs (early endosomes), Rab5 (early endosomes), Rab7 (late endosomes), LAMP1 (lysosomes), and Rab11 (recycling endosomes) (white arrowheads in Fig. 9A–E''). Thus, although the distribution of Drn did not concentrate with any particular endosomal markers, Drn appeared to localize with endocytic compartment markers, such as Hrs, Rab5, Rab7, and LAMP1, at a low frequency; this is consistent with our hypothesis that Drn plays some role in endocytic trafficking.

Drn is required for endocytic trafficking of the Dome receptor

As Drn positively contributes to JAK/STAT signaling by regulating endocytic trafficking, I speculated that Drn regulates the JAK/STAT signaling receptor Dome during its endocytic trafficking (Brown et al., 2001). I analyzed the subcellular distribution of Dome using full-length Dome protein that had a C-terminal GFP tag (Dome-GFP) and maintained wild-type Dome functions (Ghiglione et al., 2002). *UAS-dome-GFP* was ubiquitously driven under the control of *da-GAL4* in wild-type and *drn* homozygous embryos (Fig. 10A–B").

In wild-type embryos, Dome-GFP was detected in epidermal cells as punctae localized to the vicinity of the plasma membrane and cytosolic vesicles (Fig. 10A, A'; Fig. 11). Cytoplasmic vesicles containing Dome-GFP were occasionally labeled using markers of intracellular components, such as Rab5, Rab11, and LAMP1; however, Dome-GFP did not appear to associate with any particular intracellular component (Fig. 11). Previously, Dome was found to accumulate in ubiquitinated cargoes when endocytosis was impaired (Tognon

et al., 2014). Hence, whether these vesicles containing Dome-GFP were stained with an anti-ubiquitin antibody that could recognize mono- and polyubiquitin was assessed. However, almost no colocalization between Dome-DFP and ubiquitin was detected in wild-type cells (Fig. 10L–L"). In the epidermal cells of *drn*^{2} homozygotes, Dome-GFP was markedly higher than that in wild-type embryos in all cases, as observed in images of Dome-GFP obtained at the same gain of signal amplification (Fig. 10B). In images obtained using reduced gain of signal detection, Dome-GFP was observed as larger clumps located near the plasma membrane (Fig. 10B', B"). To analyze the nature of these clumps, I costained Dome-GFP with markers of representative intracellular compartments, including Pdi (ER), GM130 (*cis*-Golgi), PNA (*trans*-Golgi), Sec5 (exocytic vesicles), Hrs (early endosomes), Rab5 (early endosomes), Rab7 (late endosomes), Rab11 (recycling endosomes), and LAMP1 (lysosomes), in the epidermal cells of *drn*^{2} homozygotes. None of these markers colocalized with Dome-GFP (Fig. 10C–K"). However, large clumps of Dome-GFP often colocalized with ubiquitin (Fig. 10M–M"). The quantitative analyses revealed that 3.6% of these Dome-GFP clumps colocalized with ubiquitin and 5.3% of ubiquitin-positive vesicles colocalized with Dome-GFP. I speculated that Dome-GFP localizes with ubiquitinated cargos only temporarily because colocalization was observed only in a subset of these vesicles. Nevertheless, as ubiquitination regulates endosomal trafficking and sorting, these results suggest that Dome-GFP accumulates in atypical endosomal compartments in *drn* mutants. Such a defect in endocytosis may cause JAK/STAT signaling to deteriorate, supporting previous suggestions that endocytosis is essential for Dome activation (Devergne et al., 2007; Moore et al., 2020). Additionally, defective endocytosis may prevent the degradation of

Dome-GFP in lysosomes of *drn* mutants. Unlike Dome-GFP, the Wnt and Notch signaling receptors Frizzled2 and Notch, respectively, were unchanged in the epidermis of wild-type and drn^2 homozygotes (Fig. 12). Hence, defective endocytosis in drn^2 homozygotes is specific to Dome-GFP.

Considering the potential binding of Drn to ubiquitin, we determined whether Dome-GFP and Drn could colocalize in wild-type cells. Although the staining patterns of Drn and Dome-GFP did not broadly resemble each other, I found that Drn and Dome-GFP often colocalized with each other (white arrowheads in Fig. 10N–N"). The quantitative analyses revealed that 3.5% of Dome-GFP colocalized with Drn and 5.8% of Drn colocalized with Dome-GFP. These results suggest that Drn interacts with the ubiquitin moiety on Dome in some endocytic compartments to facilitate proper Dome trafficking. However, such an interaction may be transient because vesicles demonstrating colocalization did not account for a majority. Nevertheless, based on these results, I speculated that ubiquitinated Dome can be recognized by Drn, which can specifically promote the endocytic transportation and degradation of Dome. Dome was accumulated in the atypical endocytic compartment with ubiquitinated cargoes and JAK/STAT signaling was attenuated in *drn* mutants, indicating that such an endocytic process is crucial for activating JAK/STAT signaling (Fig. 13).

DISCUSSION

Drn contributes to the endocytic trafficking of Dome, which may be coupled with the activation of JAK/STAT signaling

In this study, I demonstrated that *drn*, which encodes a *Drosophila* ortholog of AWP1, plays crucial roles in the LR-asymmetric development of the FG and AMG by positively regulating JAK/STAT signaling. In this process, wild-type *drn* is required for the normal endocytic trafficking of Dome, which is the *Drosophila* JAK/STAT signaling receptor. Whether the internalization as well as endocytic trafficking of Dome is required to activate JAK/STAT signaling in *Drosophila* has been a topic of debate (Devergne et al., 2007; Moore et al., 2020; Ren et al., 2015; Vidal et al., 2010). Analyses of mutations affecting Dome endocytosis have revealed that Dome must be internalized into early endosomes to activate JAK/STAT signaling (Devergne et al., 2007). In contrast, the RNAi-mediated knockdown of genes required for Dome endocytosis was found to enhance JAK/STAT signaling activity, demonstrating that Dome endocytosis negatively regulates JAK/STAT signaling (Vidal et al., 2010). This discrepancy can be explained by the multiple ramifications and parallelism of the endocytic pathway, as described in recent studies (Cendrowski et al., 2016). In particular, blocking a particular step along the pathway can divert endocytic trafficking into various positive or negative regulatory cascades of cell signaling pathways. The relative contributions of endocytic regulators can also change the course of endocytic trafficking, as is well documented in Notch signaling (Shimizu et al., 2014). Moreover, a change in the balance of regulators may change how endocytosis regulates cell signaling pathways according to the context. Hence, to comprehensively understand how endocytosis contributes

to the activation of Dome, it is necessary to examine the point at which endocytosis is disrupted and the altered course of endocytic trafficking when normal endocytosis fails.

A study using RNAi of cultured *Drosophila* cells identified *drn* as a negative regulator of JAK/STAT signaling; this finding appears to be opposite to our model (Vidal et al., 2010). However, as other genes required for Dome endocytosis were also identified as negative regulators of JAK/STAT signaling in that analysis, it is likely that this discordance regarding the role of Drn in JAK/STAT signaling results from the discrepancy in the contribution of Dome endocytosis to JAK/STAT signaling, as discussed above (Cendrowski et al., 2016). Regarding this discrepancy, it has been proposed that long-term loss-of-function analyses, including analyses of mutants in which Dome endocytosis is disrupted, may reflect unexpected cell fate changes induced by altered endocytic pathways and their influence on JAK/STAT signaling (Vidal et al., 2010). However, in this study, I examined three developmental contexts in which JAK/STAT signaling is reduced in *drn* mutants. One of these involves the regulation of *eve* expression, which occurs before cell fate specification and during a short period in early embryogenesis; thus, it does not fit well with a mechanism involving unexpected cell fate changes. Therefore, I propose a model in which Drn is required in some steps of the endocytic trafficking of Dome, which plays a role in the subsequent activation of JAK/STAT signaling (Fig. 13). This model is consistent with that proposed by Devergne et al., in which the endocytic trafficking of Dome activates JAK/STAT signaling and also provides a mechanism to regulate it quantitatively (Devergne et al., 2007). However, as where and how Drn can control the endocytic trafficking of Dome

remain unclear, the coincidence between previous and current results should be interpreted with caution.

Drn is specifically involved in the endocytic trafficking of Dome

drn is the *Drosophila* ortholog of *AWP1*, which binds to ubiquitin and modulates the functions of ubiquitinated proteins in mammals and *Xenopus* species (Chang et al., 2011; Duan et al., 2000; Fenner et al., 2009; Miyata et al., 2012; Seo et al., 2013). It is known that ubiquitination of the receptors involved in JAK/STAT signaling is important for regulating signaling activities in mammals (Gesbert et al., 2005; Martinez-Moczygemba et al., 2007; Wölfler et al., 2009). The sorting of ubiquitinated membrane proteins into intraluminal vesicles relies on protein complexes in the ESCRT family (Babst et al., 2002a; Babst et al., 2002b; Katzmann et al., 2001). ESCRT-0, ESCRT-I, and ESCRT-II include multiple ubiquitin-binding proteins and interpret ubiquitin as a signal to sort membrane proteins (Clague et al., 2012). In *Drosophila* mutants of the ESCRT-0 complex components *Hrs* and *Stam*, ubiquitinated membrane proteins, such as Notch and Dome, aggregate at the cell cortex and in intracellular compartments (Jékely and Rørth, 2003; Tognon et al., 2014). As such intracellular compartments, including aggregated Dome, were stained with an anti-ubiquitin antibody, it was proposed that *Drosophila* Dome is ubiquitinated and its endosomal sorting is controlled by ubiquitination; however, the ubiquitination of Dome was not confirmed biochemically (Tognon et al., 2014). I found that a loss of Drn caused Dome to accumulate in large clumps that frequently colocalized with ubiquitin (Fig. 10M–M") but were not labeled by markers of typical intracellular compartments (Fig. 10C–K"). In addition, Drn

occasionally colocalized with markers of various endocytic compartments, demonstrating that Drn is an endocytic protein (Fig. 9). Hence, I speculated that Drn plays a role in the ubiquitin-dependent internalization or sorting of Dome through its potential ubiquitin-binding activity (Fig. 13). This idea is consistent with my observation that Drn often colocalizes with Dome in some intracellular vesicles in wild-type *Drosophila* (Fig. 10N–N"). Thus, in this model, Dome may be misrouted to atypical endocytic compartments, where it fails to be phosphorylated in the absence of Drn. Conversely, differences in Dome trafficking routes between wild-type and *drn* mutant embryos should help identify the endocytic compartment where Dome is activated by phosphorylation. However, it is difficult to delineate incorrect Dome trafficking routes in the *drn* mutant because Dome did not specifically colocalize with typical markers of endocytic compartments under this condition. This model also predicts that such misrouting can consequently prevent the degradation of Dome in lysosomes and leave it to accumulate, as observed in *drn* mutants (Fig. 13).

My analyses revealed that *drn* mutations induced marked accumulation of Dome but not of Notch or Fz2 (Fig. 12). The intracellular distribution of Notch and Fz2 in the *drn* mutant appeared to be similar to that in the wild type. Thus, Drn is not a general component of endosomal protein sorting but is specific to Dome; however, how such specificity is achieved remains unclear.

Roles of JAK/STAT signaling in LR-asymmetric development of the *Drosophila* gut

In this study, I found that JAK/STAT signaling activity must be maintained at proper levels for normal LR-asymmetric development of the FG and AMG. Previously, a similar

phenomenon in Wnt or JNK signaling activity was observed (Kuroda et al., 2012; Taniguchi et al., 2007). However, this study and previous research failed to detect any LR asymmetry in the activity or the distribution of molecules involved in the JAK/STAT, Wnt, and JNK signaling pathways (Fig. 7) (Kuroda et al., 2012; Taniguchi et al., 2007). As these three signaling pathways are required for LR-asymmetric rearrangement of nuclei in the visceral muscles of the MG, they may play permissive roles in rearranging these nuclei upon a common cue, which is yet unknown, of LR polarity.

AWP1/Drn is highly conserved from *Drosophila* to humans (Fig. 1E). As receptors in the mammalian JAK/STAT pathway are also ubiquitinated, I speculated that the role of AWP1/Drn in JAK/STAT signaling and LR-asymmetric development is evolutionarily conserved in various organisms (Gesbert et al., 2005; Martinez-Moczygemba et al., 2007; Wölfler et al., 2009).

MATERIALS AND METHODS

Fly stocks

Canton-S was used as the wild-type *Drosophila* strain. drn^{1}, and drn^{2} mutants were generated for this study by previous graduate students of the Matsuno laboratory. $drn^{GS12294}$ and $drn^{GS10567}$ are previously reported GS lines (Toba et al., 1998). *UAS-drn*, and *UAS-myc-drn* were also generated in this study. *UAS-hop*^{Tuml} (Harrison et al., 1995) and *UAS-dome-GFP* (Ghiglione et al., 2002) have been previously described. *UAS-drnRNAi* (VDRC#103508) was used for RNAi against *drn*. The following GAL4 lines were used in this study: *da-GAL4* (Wodarz et al., 1995), *48Y-GAL4* (Martin-Bermudo et al., 1997), *24B-GAL4* (Brand and Perrimon, 1993), *hand-GAL4* (Popichenko et al., 2007), *elav-GAL4* (Yao and White, 1994), *NP1522* (Hayashi et al., 2002), *NP5021* (Hayashi et al., 2002), *NP0221* (Hayashi et al., 2002), and *65E04* (Jenett et al., 2012). The lines used to generate homozygotes of drn^{2} lacking its maternal contribution were *P{ry*$^{+t7.2}$*=neoFRT}82B ry*^{506} (Bloomington #2035) and *w***;P{ry*$^{+t7.2}$*=neoFRT}82B P{w*$^{+mC}$*=ovoD1-18}3R/st*^{1}*βTub85D*^{D}*ss*^{1}*e*^{s}*/TM3, Sb*^{1} (DGRC#106675).

All fly stocks were maintained on standard *Drosophila* medium at 25°C, unless stated otherwise. Mutant alleles of the second and third chromosomes were balanced with appropriate blue balancers, such as *CyO, P{en1}wg*^{en11}, *TM6B, AbdA-lacZ*, and *TM3, ftz-lacZ*.

Generation of drn^{1} and drn^{2} mutants

The *drn*-deletion mutants drn^{1} and drn^{2} were generated by imprecise excision of P elements from *GS12689* and *GS10487*, respectively (Toba et al., 1998). Imprecise excision was

performed using a standard procedure described previously (Hummel and Klämbt, 2008). *drn*^{1} and *drn*^{2} mutations contain deletions from 9,353,341 to 9,355,167 and from 9,353,293 to 9,358,171, respectively (FlyBase2015_03, Dmel Release 6.06). The flies mentioned above were generated by previous graduate students Reo Maeda and Junpei Kuroda.

Generation of homozygotes for *drn* lacking maternal contribution

drn^{2} homozygous embryos lacking the *drn* maternal contribution (*drn*$^{2\ m/z}$) were obtained using standard crosses described previously (Prudencio and Guilgur, 2015). In brief, *FRT82B* was introduced into the *drn*^{2} chromosome by recombination. Flies carrying *FRT82B drn*^{2} were selected by Geneticin (Gibco) and genomic PCR using the primers 5′-TCACGCATTCAGAGCTTCGTGTGCCC-3′ and 5′-ATGTTGCTGCGTTTGCTCTGCGTATTCCAC-3′. *FRT82B drn*^{2}*/TM3b, Sb* females were crossed with *hsFLP/Y; FRT82B ovoD/TM3, Sb* males to obtain *hsFLP/+; FRT82B ovoD/FRT82B drn*^{2} females through heat-shock treatment. These females were then crossed with *FRT82B drn*^{2}*/TM3b, Sb* males, and heat-shock treatment was performed again to obtain *FRT82B drn*^{2} homozygous embryos without the *drn* maternal contribution.

Generation of UAS-*drn* and UAS-*myc-drn* transgenic flies

To construct *UAS-drn*, a cDNA fragment composed of an entire open reading frame of a *drn* transcript (CG45050-RC) was PCR amplified using an upper strand primer containing an *EcoRI* site (5′-CCGGAATTCAGCAGGAAGCAGACGAAACT-3′) and a lower-strand primer containing *HindIII* and *BglII* sites (5′-

CCCCAAGCTTAGATCTTCCTTGTTATAGCGCAGCAT-3′). The cDNA clone RE70963 was used as a template (Stapleton et al., 2002). The PCR product was digested with *EcoRI* and *HindIII*, subcloned into the *EcoRI* and *HindIII* sites of pBluescript, and sequenced (Agilent Technologies). The cloned fragment was subcloned into the *EcoRI* and *BglII* sites of the pUAST vector (Brand and Perrimon, 1993).

To construct UAS-*myc-drn*, a DNA fragment composed of an entire open reading frame of a *drn* transcript (CG45050-RC) was PCR amplified using RE70963 cDNA as a template, an upper strand primer containing *EcoRI* and *BglII* sites and the *myc*-tag coding sequence (underlined) (5′-CCGGAATTCCAAAATGGAGCAGAAGCTGATCTCGGAGGAGGATCTGAGATCTATGGAACGTGAATCTAACCC-3′), and a lower strand primer containing a *XhoI* site (5′-CCGCTCGAGTCAAATCTTTTGAATCTTCT-3′). CG45050-RC has the same open reading frame as CG45050-RB, -RD, -RE, -RF, and -RG (Fig. 1D). The PCR product was digested with *EcoRI* and *XhoI* and subcloned into pUAST. The DNA sequence of the coding region was then confirmed. UAS-*drn* and UAS-*myc-drn* constructs were introduced into the *Drosophila* genome using P element-mediated transformation (Spradling and Rubin, 1982). The flies mentioned above were generated by previous graduate students Reo Maeda and Junpei Kuroda.

Generation of an anti-Drn antibody

A fragment of *drn* cDNA (RE70963) containing an entire open reading frame of CG45050-RC was amplified by PCR, sequenced, and subcloned into the *BamHI* and *EcoRI* sites of the

pGEX-2T vector (GE Healthcare Life Sciences). A GST-Drn fusion protein was produced in Origami B (DE3) cells (Novagen) and purified using a Glutathione Sepharose 4B column. The purified GST-Drn fusion protein was used to immunize rats, and polyclonal antiserum was purified using a standard protocol.

Antibody staining, *in situ* hybridization, and microscopic analysis

Embryos were immunostained as described previously using the following primary antibodies: mouse anti-Fas3 (1:100, DSHB, 7G10), chicken anti-β-galactosidase (1:500, Abcam, ab9361), mouse anti-Pdi (1:200, Stressgen, 1D3), anti-lectin-PNA (1:500, Vector Laboratories), mouse anti-Sec5 (1:200, 22A2; Murthy et al., 2003), rabbit anti-GM130 (1:50, Abcam, ab30637), guinea pig anti-Rab5 (1:3000, gift from Akira Nakamura), rabbit anti-Rab7 (1:5000; Tanaka and Nakamura, 2008), rabbit anti-Rab11 (1:5000; Tanaka and Nakamura, 2008), guinea pig anti-Hrs (1:1000; Lloyd et al., 2002), mouse anti-multiubiquitin antibody (1:200, MBL, FK2), rabbit anti-LAMP1 antibody (1:1000, Abcam, ab30687), mouse anti-extra domain of Notch (1:500, DSHB, C458.2H), mouse anti-Frizzled2 (1:20, DSHB, 1A3G4), rabbit anti-GFP (1:500, MBL, 598), rabbit anti-RFP (1:500, MBL, PM005), rat anti-GFP (1:500, Nacalai Tesque, 04404-26), mouse anti-eve (1:20, DSHB, 3C10), and rat anti-Drn (1:500). The chitin-binding probe CBP546 was prepared from a bacterial expression construct using the protocol provided by Yinhua Zhang (New England Biolabs) (Dong et al., 2014). CBP546 (1:50) was added along with secondary antibodies for other primary antibodies to perform trachea staining. Images were obtained using an LSM880 (Carl Zeiss) microscope and processed using Adobe Photoshop. For *in situ* hybridization, standard

protocols were used, as described previously (Jiang et al., 1991). Images were obtained using an Axiosop2 Plus (Carl Zeiss) microscope.

Quantitative analyses of colocalizations in intracellular vesicles

The same threshold was set for each pair of images (two channels representing respective markers) using ImageJ. Using the Analyze Particles function, particles larger than five-pixel units were defied as the region of interest (Roi). Roi sets from two channels of an image were compared. Each Roi overlapping between two channels was defined as a particle demonstrating colocalization and was used for calculating the colocalization rate between two markers. The number of Rois showing colocalization against the total number of Rois was calculated as the percentage of colocalization.

FIGURES

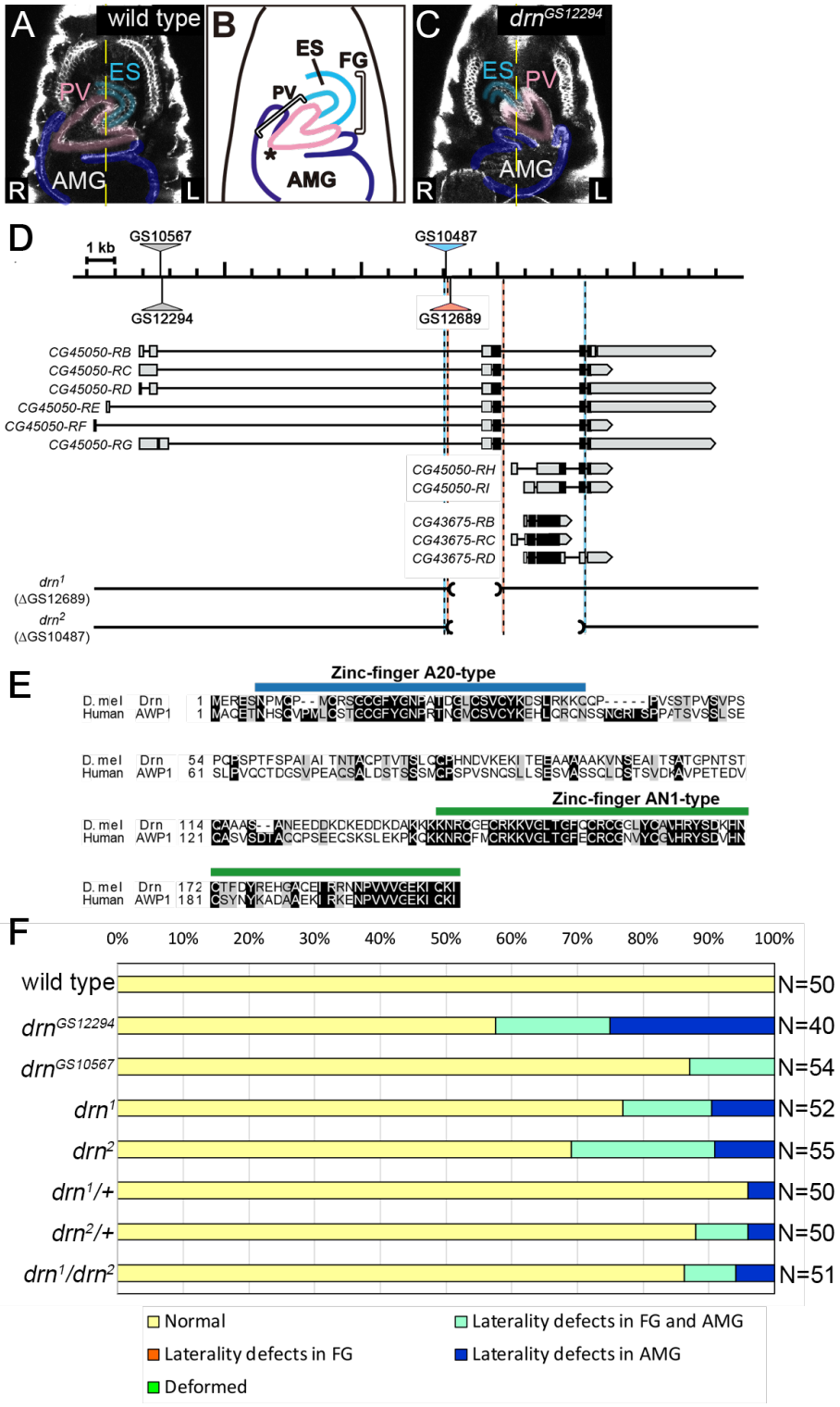
A
wild type
ES
PV
AMG
R
L
B
ES
FG
PV
AMG
C
drnGS12294
ES
PV
AMG
R
L
D
1 kb
GS10567
GS10487
GS12294
GS12689
CG45050-RB
CG45050-RC
CG45050-RD
CG45050-RE
CG45050-RF
CG45050-RG
CG45050-RH
CG45050-RI
CG43675-RB
CG43675-RC
CG43675-RD
drn1 (ΔGS12689)
drn2 (ΔGS10487)
E
Zinc-finger A20-type
Zinc-finger AN1-type
D. mel Drn
Human AWP1
F
0%
10%
20%
30%
40%
50%
60%
70%
80%
90%
100%
wild type
drnGS12294
drnGS10567
drn1
drn2
drn1/+
drn2/+
drn1/drn2
N=50
N=40
N=54
N=52
N=55
N=50
N=50
N=51
Normal
Laterality defects in FG and AMG
Laterality defects in FG
Laterality defects in AMG
Deformed

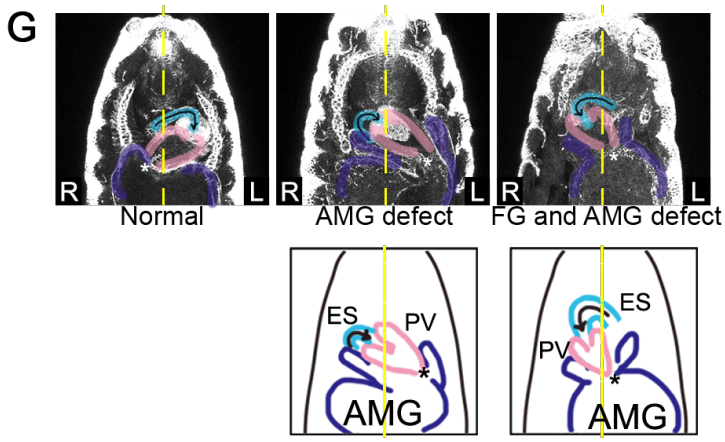

Figure 1. LR asymmetry of the FG and AMG is defective in *drn* mutants

(A) Ventral view of a stage 16 wild-type embryo. The gut outline was visualized by anti-Fas3 immunostaining. LR asymmetry of the FG was judged by the direction of ES (turquoise) rotation and that of the AMG was judged by the position of the joint (asterisk) between the AMG (dark blue) and PV (pink) relative to the midline (yellow dotted line). (B) A diagram of the FG and AMG in wild-type embryos at stage 16, depicting the ES, PV, and AMG. (C) LR inversion of the FG and AMG in $drn^{GS12294}$ homozygotes. Symbols are the same as those in A. (D) A diagram showing the genomic region of *drn* (upper), its alternative transcripts (middle), and the structures of drn^{1} and drn^{2} mutants (lower) with P element insertion sites (triangles), deleted regions (parentheses and dotted lines), exons corresponding to coding regions (black boxes), untranslated regions (gray boxes), and introns (lines). (E) Amino acid sequences of *Drosophila* Drn (NP_001027162.1) and human AWP1 (NP_061879) were optimally aligned using ClustalW. The diagram indicates identical (white characters on black) and similar residues (black characters on gray). A20-type and AN1-type zinc finger domains are indicated by blue and green lines, respectively. (F) The frequency of FG and AMG LR

defects (%) in embryos with the genotypes indicated on the left. Bars denote the percentage of embryos with no laterality defects (yellow), with laterality defects in only the FG (orange) or the AMG (blue), or in both the FG and AMG (turquoise), or with deformities (green). The number (N) of embryos scored is shown on the right. (G) Examples of LR asymmetry phenotypes in the FG and AMG in *drn*^{2} homozygotes. Schematic diagrams representing LR defects are presented below. The ES (turquoise), PV (pink), and midline (yellow dotted line) are as described in A. L and R represent the left and right sides of embryos, respectively.

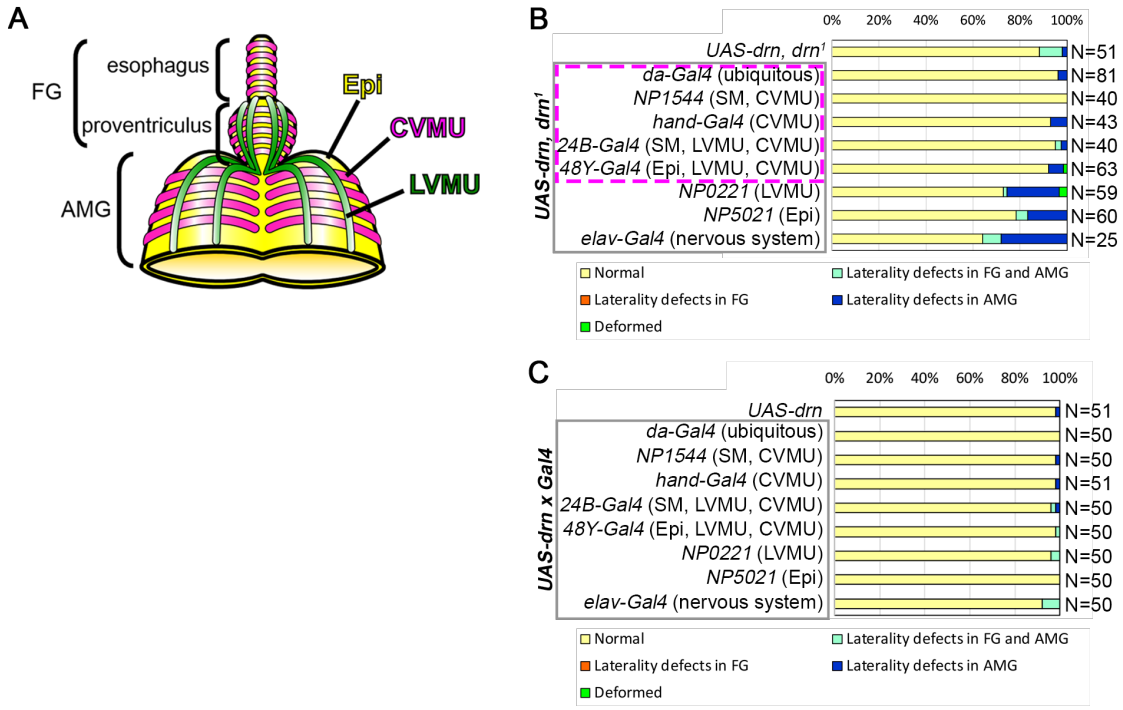

Figure 2. *drn* is required in the CVMU of the midgut for LR-asymmetric development of the FG and AMG.

(A) A diagram of the visceral muscles after stage 14: the FG and AMG are overlaid by a layer of CVMU (magenta), and the PV and AMG are covered by LVMU (green). The epithelium is shown in yellow. (B) The frequency of LR asymmetry defects (%) in the FG and AMG in embryos carrying *UAS-drn*, drn^1/drn^1 without (control, *UAS-drn*, drn^1) or with the GAL4 drivers outlined in gray on the left. *GAL4* expression was driven in the cell types or tissues shown in parentheses (SM: somatic muscles; Epi: epithelium of the AMG). Bars denote the percentage of embryos with no laterality defects (yellow), with laterality defects in only the FG (orange) or the AMG (blue), or in both the FG and AMG (turquoise), or with deformities (green). *UAS-drn* misexpression driven by the GAL4 drivers outlined in magenta rescued the laterality defects. The number (N) of embryos scored is shown on the right. (C)

The frequency of LR asymmetry defects (%) in the FG and AMG of embryos carrying *UAS-drn* without any GAL4 driver (control, *UAS-drn*) or with the respective GAL4 drivers shown on the left. Bars denote the percentage of embryos with no laterality defects (yellow), with laterality defects in only the FG (orange) or the AMG (blue), or in both the FG and AMG (turquoise), or with deformities (green). The number (N) of embryos scored is shown on the right.

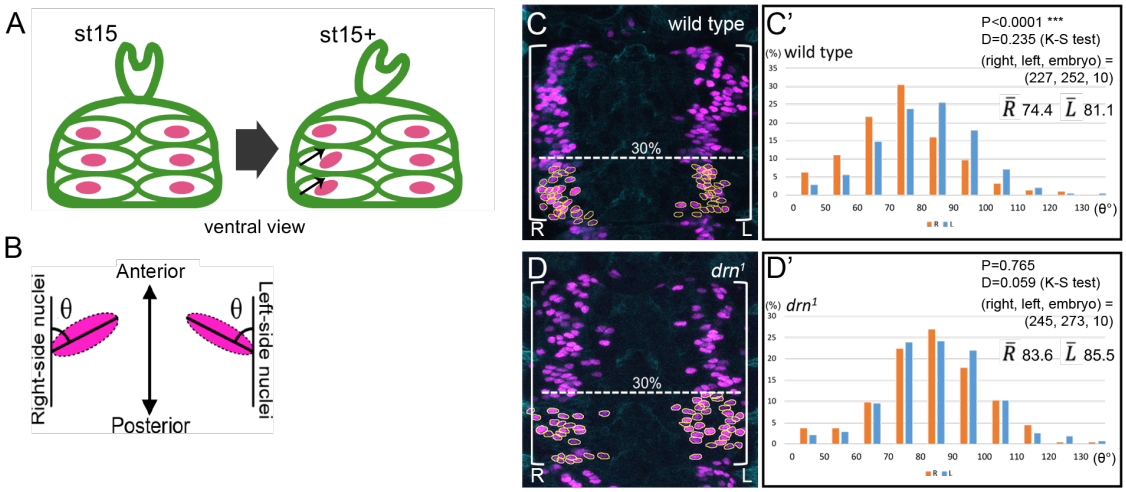

Figure 3. *drn* is required for the LR asymmetric rearrangement of CVMU cells during AMG development.

(A) A diagram showing the LR-asymmetric rearrangement of nuclei (magenta) in CVMU cells (green ellipses) of the AMG from early (st15) to late stage 15 (st15+). Small arrows indicate the tilt of the ellipsoid nuclei. (B) A diagram showing the major axis angles of the ellipsoid nuclei, represented by the angle (θ) between the major axis of the right- and left-side ellipsoid nuclei and the anterior–posterior axis of the embryo. (C and D) Ventral views of the AMG showing CVMU cells and their nuclei, stained by anti-Fas3 (cyan) and anti-RFP (magenta) antibodies, respectively, in control (C, *65E04-GAL4/UAS-Redstinger*) and *drn*^{1} homozygous (D, *drn*^{1}, *65E04-GAL4/drn*^{1}, *UAS-Redstinger*) embryos at late stage 15. Nuclei in the lower 30% of the presumptive first chamber (indicated by white angle brackets) were selected for measurement (encircled by yellow lines). (C', D') Frequency histograms of the axis angles (in 10° increments) on the left (blue bars) and right (orange bars) sides of CVMU cell nuclei in the ventral AMG of control (C', *65E04-GAL4/UAS-Redstinger*) and *drn*^{1} homozygous (D', *drn*^{1}, *65E04-GAL4/drn*^{1}, *UAS-Redstinger*) embryos at late stage 15. *P*

values (upper right corner) indicate the statistical significance of differences between the angle distributions on the right and left sides calculated using the K–S test. Numbers in parentheses indicate the numbers (right nuclei, left nuclei, and embryos) analyzed. The average angles on the right and left sides are indicated as $\overline{R}$ and $\overline{L}$, respectively. In C and D, L and R represent the left and right sides of embryos, respectively.

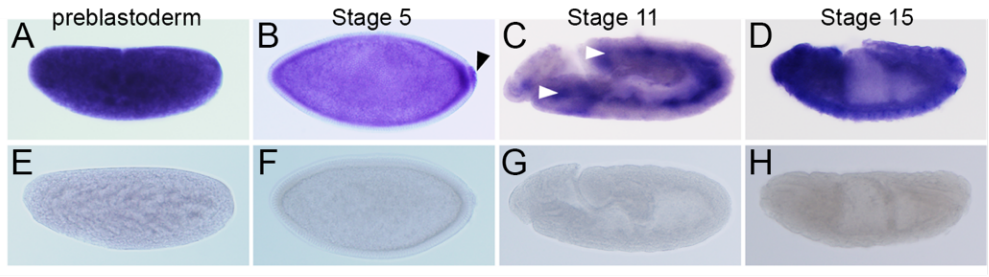

Figure 4. *drn* expression is detected by *in situ* hybridization at various embryonic stages. (A–H) Whole-mount *in situ* hybridization with anti-sense (A–D) and sense RNA probes (E–H) against *drn* at the preblastoderm stage (A, E), stage 5 (B, F), stage 11 (C, G), and stage 15 (D, H) of wild-type embryos. The black arrowhead in B indicates pole cells. White arrowheads in C indicate the TVM.

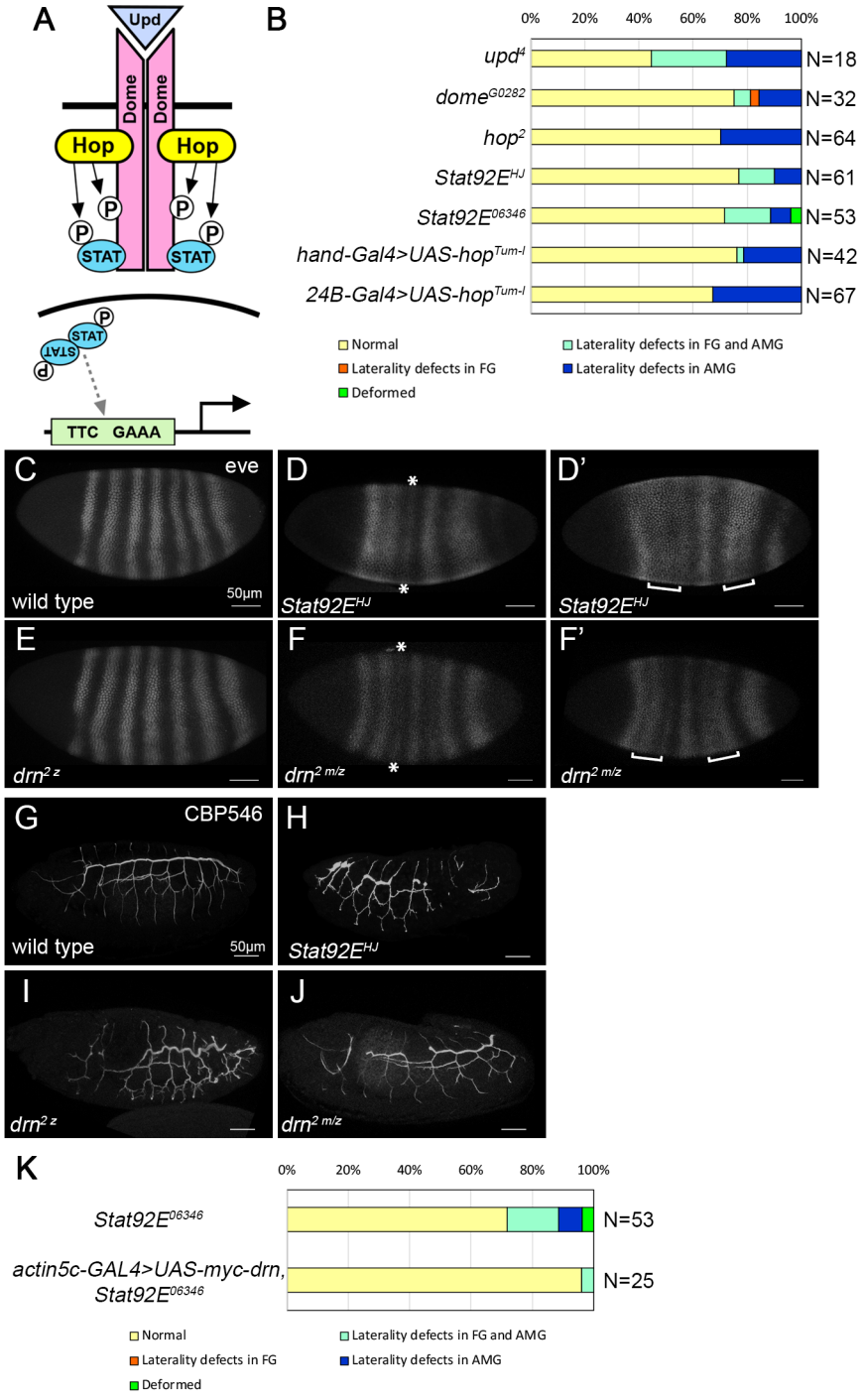

Figure 5. *drn* functions collectively with JAK/STAT signaling during embryonic development.

(A) Illustration of the *Drosophila* JAK/STAT pathway. (B) The frequency of LR asymmetry defects (%) in the FG and AMG of embryos with the genotypes indicated on the left. Bars denote the percentage of embryos with no laterality defects (yellow), with laterality defects in only the FG (orange) or the AMG (blue), or in both the FG and AMG (turquoise), or with deformities (green). The number (N) of embryos scored is shown on the right. (C–F') The expression of *even-skipped* in wild-type (C), $Stat92E^{HJ}$ (D and D'), $drn^{2\ z}$ (zygotic mutant) (E), and $drn^{2\ m/z}$ (zygotic and maternal mutant) (F and F') embryos. D and F show the phenotype of weakened stripe 3 (marked with asterisks). D' and F' show the phenotype of stripe fusion (marked with brackets). (G–J) The trachea was detected by CBP546 staining in wild-type (G), $Stat92E^{HJ}$ (H), $drn^{2\ z}$ (zygotic mutant) (I), and $drn^{2\ m/z}$ (zygotic and maternal mutant) (J) embryos. (K) The frequency of LR asymmetry defects (%) observed in the FG and AMG of $Stat92E^{06346}$ homozygotes without (control, upper) and with ubiquitous misexpression of *UAS-myc-drn* driven by *actin5c-GAL4* (lower). Bars denote the percentage of embryos with no laterality defects (yellow), with laterality defects in only the FG (orange) or the AMG (blue), or in both the FG and AMG (turquoise), or with deformities (green). The number (N) of embryos scored is shown on the right. Scale bars in C–J: 50 μm.

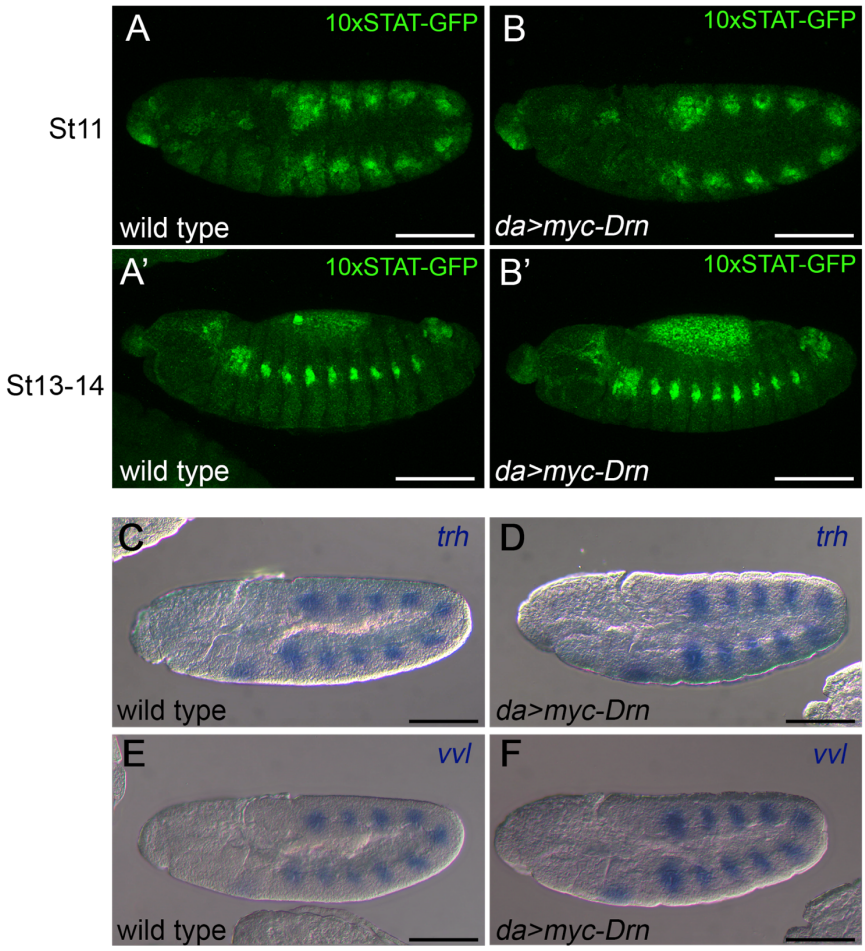

Figure 6. The activity of JAK/STAT signaling remains unchanged upon upregulation of *drn*.

(A–B') Expression pattern of 10xSTAT-GFP in wild-type (A and A') and da-GAL4 driven overexpression of myc-Drn (B' and B') at the embryonic stages noted on the left side. (C-F) Whole-mount *in situ* hybridized wild-type and da-GAL4 driven myc-Drn overexpressed embryos with anti-sense *trh* (C and D) and *vvl* (E and F) RNA probes. Scale bar: 100 μm.

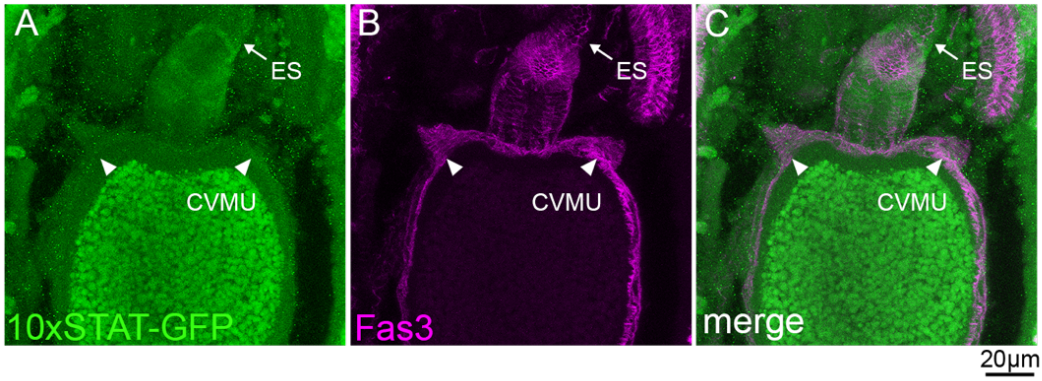

Figure 7. JAK/STAT signaling activity in the AMG has no obvious LR asymmetry.

(A–C) JAK/STAT signaling in the FG and AMG, detected by the reporter gene *10×STAT-GFP* (green in A, C), at stage 15 in wild-type embryos (ventral view). GFP derived from *10×STAT-GFP* was detected by anti-GFP antibody staining. The visceral muscles overlaying the PV and AMG were detected by anti-Fas3 antibody staining (magenta in B, C). (C) Merged images of panels A and B. Arrows and arrowheads denote the activation of *10×STAT-GFP* in the ES and CVMU, respectively. Scale bar: 20 μm.

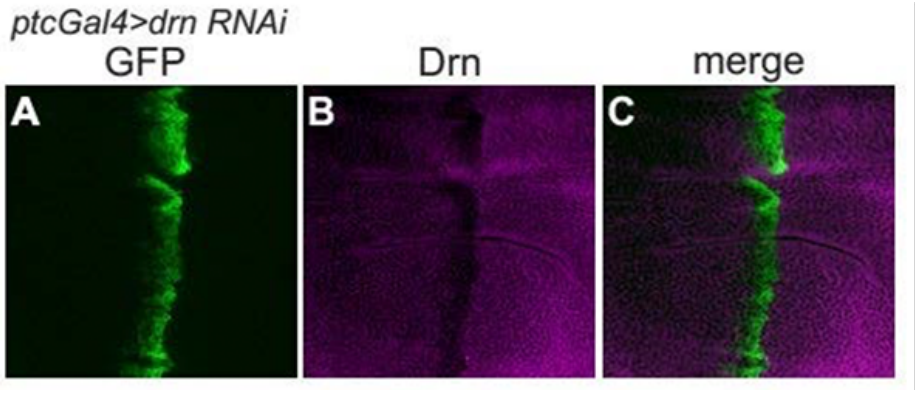

Figure 8. Anti-Drn antibody specifically detects endogenous Drn.

(A-C) In the wing discs of third-instar larvae, *drn* gene was knocked down by RNAi under the control of *ptc-GAL4* where *UAS-GFP* was expressed (green in A, C). These wing discs were stained with anti-Drn antibody (magenta in B, C). C shows a merged image of A and B.

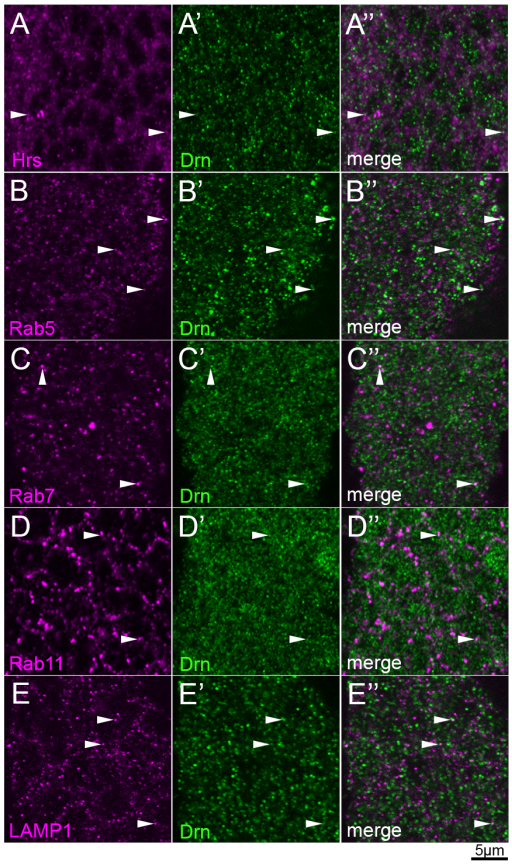

Figure 9. Drn occasionally colocalizes with markers of various endocytic compartments in the epidermis of wild-type embryos.

(A–E") Drn subcellular localization in the epidermal cells of wild-type embryos. Embryos were double stained with anti-Drn (green, middle and right columns) and the following endosomal markers (magenta, left and right columns): (A and A") Hrs (early endosomes), (B and B") Rab5 (early endosomes), (C and C") Rab7 (late endosomes), (D and D") Rab11 (recycling endosomes), and (E and E") LAMP1 (lysosomes). A"–E" show merged images of A–E and A'–E', in the given order. White arrowheads indicate vesicles showing the colocalization of Drn with markers of various endocytic compartments. Scale bar: 5 μm.

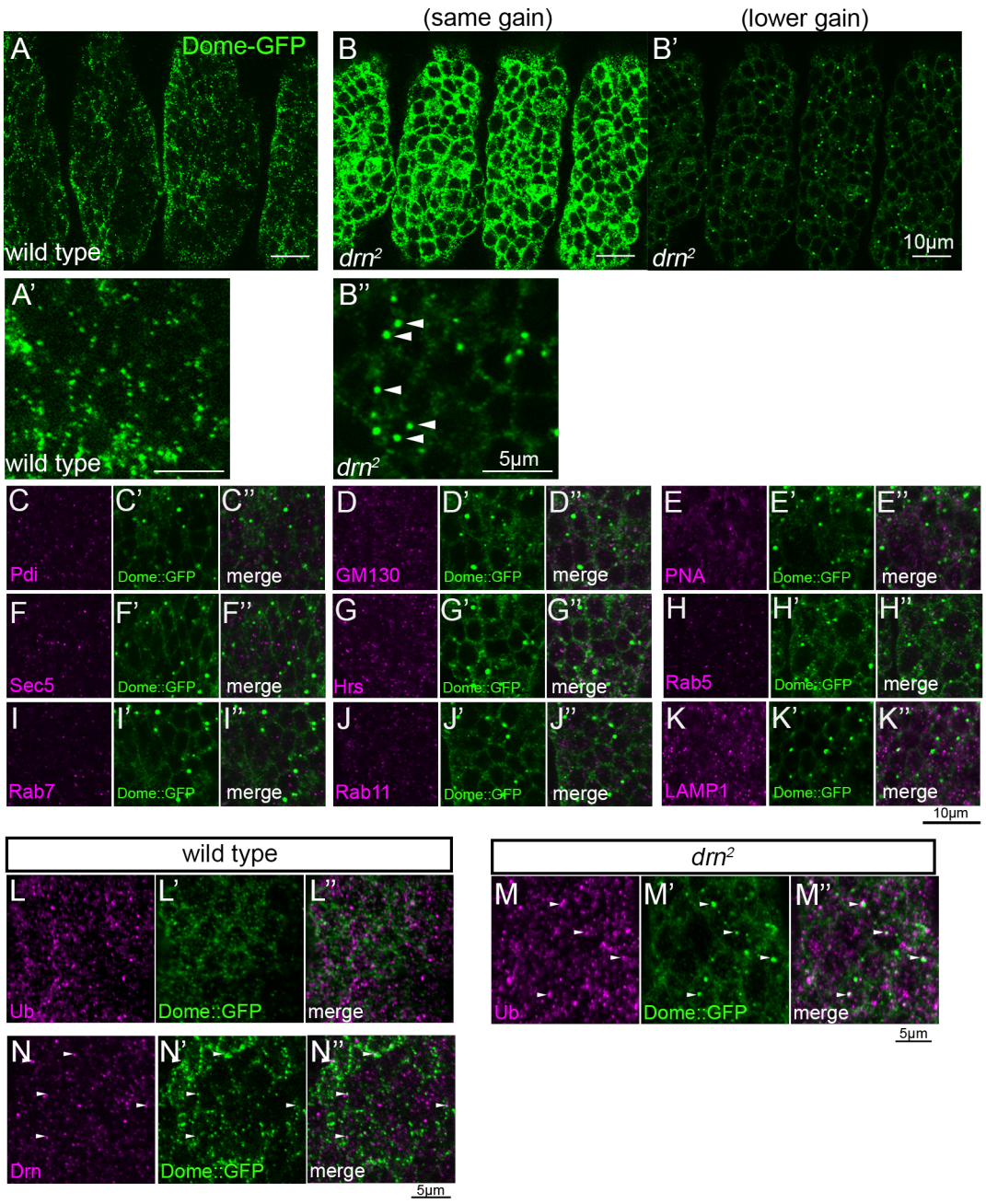

Figure 10. Dome accumulated in the cell cortex and intracellular structures in the epidermis of *drn* mutant embryos.

(A–B'') Ubiquitous *UAS-dome-GFP* expression was driven by *da-GAL4.* Dome-GFP was detected by anti-GFP antibody staining in the epidermal cells of wild-type (A) and *drn*^{2} (B-B'') embryos. Gain to capture was the same for images in A, A', and B. Images in B' and B" use a lower gain to visualize intracellular aggregations and avoid signal saturation. A' and B" are magnified views of A and B'. White arrowheads in B" indicate Dome-GFP aggregations. Scale bars: 10 μm in A–B' and 5 μm in A' and B". (C–K") The subcellular localization of Dome-GFP aggregates in epidermal cells of *drn*^{2} mutants. Embryos were double stained with anti-GFP antibody (green, middle and right columns) and antibodies against the following markers of intracellular compartments (magenta, left and right columns): (C, C") Pdi (ER), (D, D") GM130 (*cis*-Golgi), (E, E") PNA (*trans*-Golgi), (F, F") Sec5 (exocyst), (G, G") Hrs (early endosomes), (H, H") Rab5 (early endosomes), (I, I") Rab7 (late endosomes), (J, J") Rab11 (recycling endosomes), and (K, K") LAMP1 (lysosomes). C"–K" show merged images of C–K and C'–K', in the given order. Scale bar: 10 μm. (L–M'') The expression of *UAS-dome-GFP* was ubiquitously driven by *da-GAL4* in wild-type (L–L") and *drn*^{2} mutant (M–M") embryos. Dome-GFP and ubiquitinylated proteins were detected by anti-GFP (green, L', L", M', and M") and anti-ubiquitin (Ub) (magenta, L, L", M, and M") antibody staining, respectively, in epidermal cells. L" and M'' are merged images of L–L' and M–M', respectively. White arrowheads denote vesicles showing colocalization between aggregated Dome-GFP and Ub in *drn*^{2}. Scale bar: 5 μm. (N–N'') The expression of *UAS-dome-GFP* was ubiquitously driven by *da-GAL4* in the wild type. Dome-GFP and Drn were detected by anti-GFP (green, N' and N") and anti-Drn (magenta, N and N") antibody staining, respectively,

in epidermal cells. N" is a merged image of N and N'. White arrowheads denote vesicles showing colocalization between Dome-GFP and Drn. Scale bar: 5 μm.

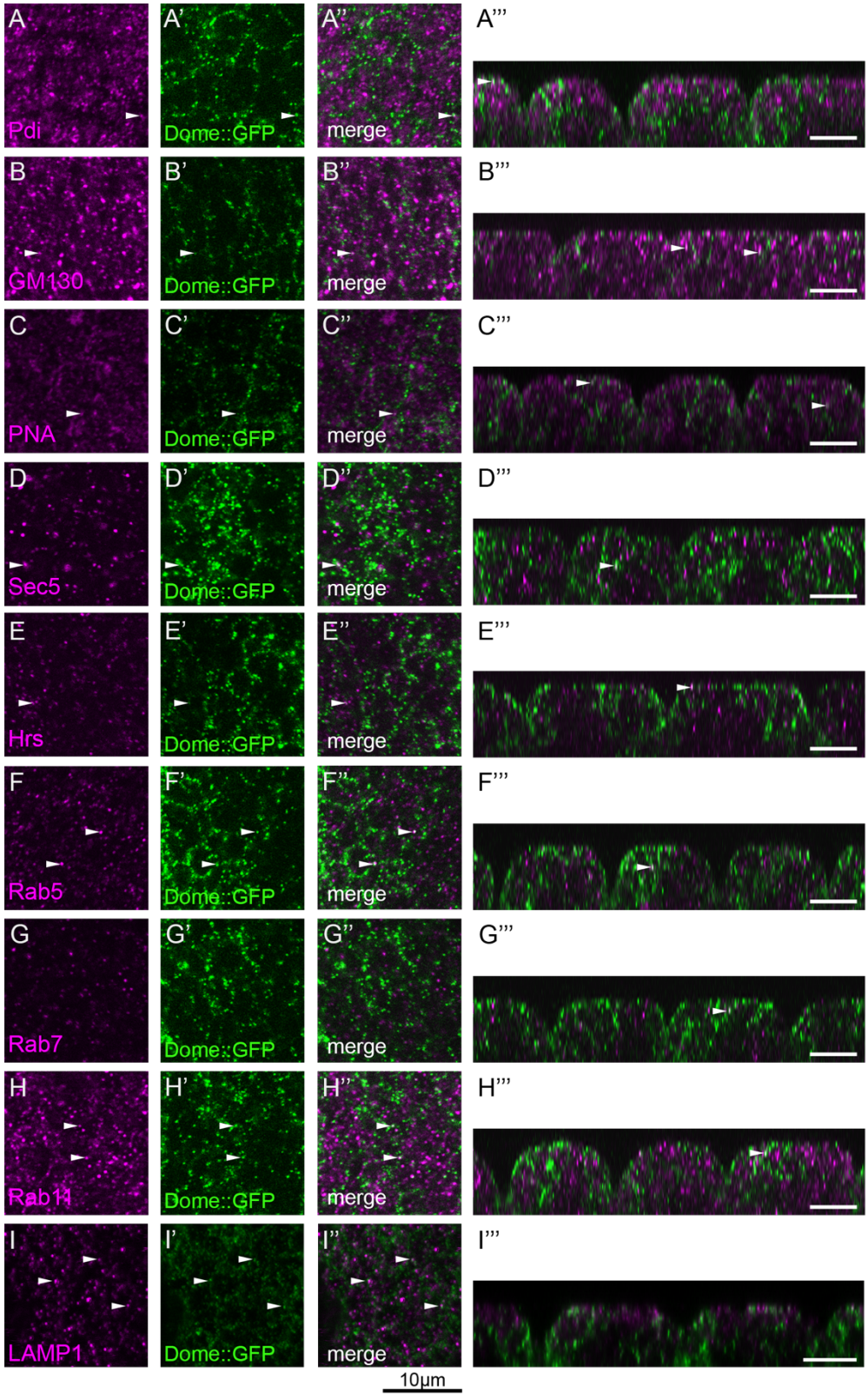
A
A'
A''
A'''
Pdi
Dome::GFP
merge
B
B'
B''
B'''
GM130
Dome::GFP
merge
C
C'
C''
C'''
PNA
Dome::GFP
merge
D
D'
D''
D'''
Sec5
Dome::GFP
merge
E
E'
E''
E'''
Hrs
Dome::GFP
merge
F
F'
F''
F'''
Rab5
Dome::GFP
merge
G
G'
G''
G'''
Rab7
Dome::GFP
merge
H
H'
H''
H'''
Rab11
Dome::GFP
merge
I
I'
I''
I'''
LAMP1
Dome::GFP
merge
10μm

Figure 11. Dome occasionally colocalizes with markers of various endocytic compartments in the epidermis of wild-type embryos.

(A–I”’) Dome subcellular localization in the epidermal cells of wild-type embryos. Embryos were double stained with anti-GFP antibody (green, middle and right columns) and against the following markers of intracellular compartments (magenta, left and right columns): (A–A”’) Pdi (ER), (B–B”’) GM130 (*cis*-Golgi), (C–C”’) PNA (*trans*-Golgi), (D–D”’) Sec5 (exocyst), (E–E”’) Hrs (early endosomes), (F–F”’) Rab5 (early endosomes), (G–G”’) Rab7 (late endosomes), (H–H”’) Rab11 (recycling endosomes), and (I–I”’) LAMP1 (lysosome). (A”–I”) Merged images of A–I and A’–I’, in the given order. A”’–I”’ shows sagittal sections from A”–I”, in the given order. White arrowheads indicate vesicles showing the colocalization of Dome with markers of various endocytic compartments. Scale bar: 10 μm.

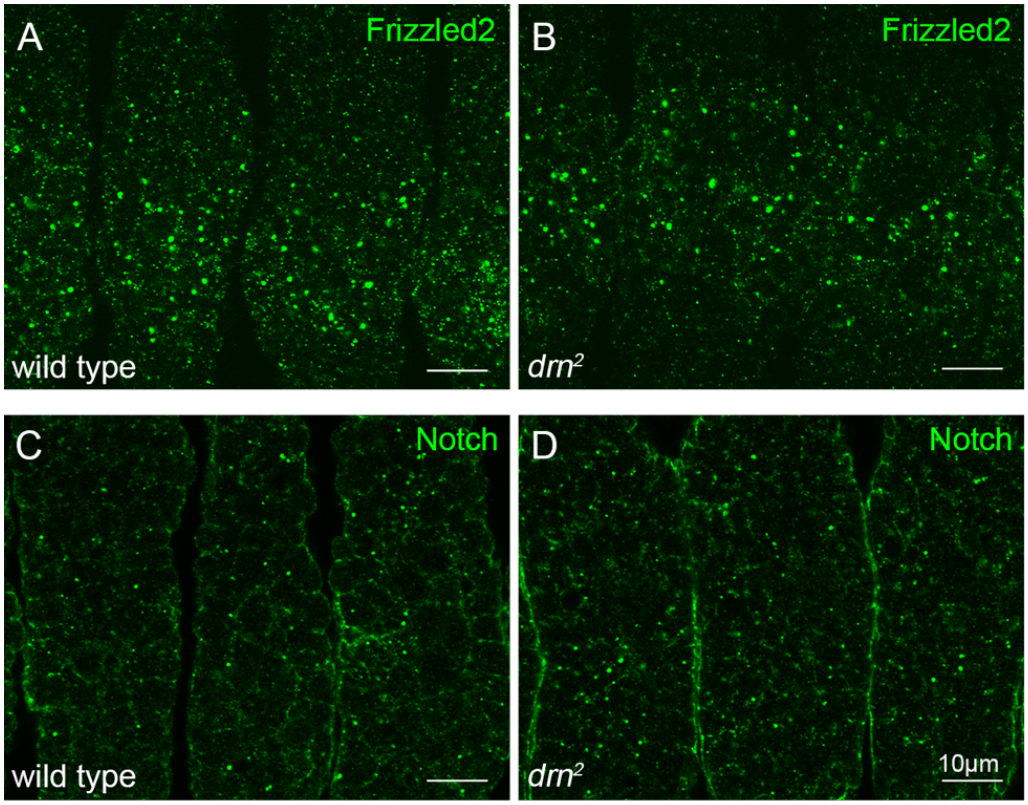

Figure 12. Drn is not required for proper Fz2 or Notch trafficking.

(A-D) The distribution of Fz2 and Notch, detected by anti-Fz2 (A and B) and anti-Notch (C and D) antibody staining, in the epidermis of wild-type (A, C) or *drn*^{2} homozygous (B, D) embryos. Scale bar: 10 µm.

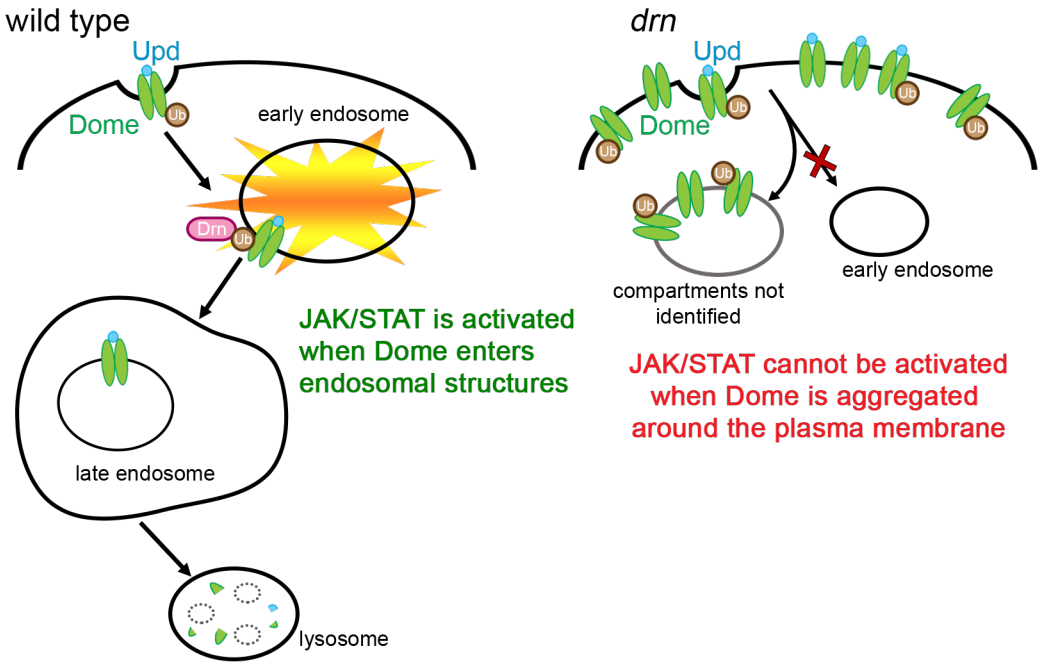

Figure 13. Drn is required for Dome endocytosis, which contributes to the activation of JAK/STAT signaling.

A schematic diagram showing the potential role of Drn in the endocytic trafficking of Dome. In the presence of Drn, ubiquitinated Dome is transported to late endosomes through the endocytic pathway. The interaction of Drn with ubiquitinated Dome may be required for the internalization of Dome, a process that enables the activation of Dome and STAT. Such internalization is also required for the proper degradation of Dome in lysosomes. In contrast, in the absence of Drn, Dome fails to properly proceed in the endocytic trafficking pathway, which attenuates JAK/STAT signaling activity. Moreover, the failure of endocytosis leads to the abnormal accumulation of Dome in atypical endocytic compartments containing ubiquitin, which are yet to be identified.

REFERENCES

Agaisse, H., Petersen, U.-M., Boutros, M., Mathey-Prevot, B. and Perrimon, N. (2003). Signaling Role of Hemocytes in *Drosophila* JAK/STAT-Dependent Response to Septic Injury. *Dev Cell* **5**, 441–450.

Arbouzova, N. I. and Zeidler, M. P. (2006). JAK/STAT signalling in *Drosophila*: insights into conserved regulatory and cellular functions. *Development* **133**, 2605–2616.

Arendt, D. and Nübler-Jung, K. (1997). Dorsal or ventral: Similarities in fate maps and gastrulation patterns in annelids, arthropods and chordates. *Mech Dev* **61**, 7–21.

Babst, M., Katzmann, D. J., Snyder, W. B., Wendland, B. and Emr, S. D. (2002a). Endosome-Associated Complex, ESCRT-II, Recruits Transport Machinery for Protein Sorting at the Multivesicular Body. *Dev Cell* **3**, 283–289.

Babst, M., Katzmann, D. J., Estepa-Sabal, E. J., Meerloo, T. and Emr, S. D. (2002b). Escrt-III: An endosome-associated heterooligomeric protein complex required for MVB sorting. *Dev Cell* **3**, 271–282.

Bach, E. A., Ekas, L. A., Ayala-Camargo, A., Flaherty, M. S., Lee, H., Perrimon, N. and Baeg, G.-H. (2007). GFP reporters detect the activation of the *Drosophila* JAK/STAT pathway in vivo. *Gene Expr Patterns* **7**, 323–331.

Baum, B. (2006). Left–Right Asymmetry: Actin–Myosin through the Looking Glass. *Curr Biol* **16**, R502–R504.

Binari, R. and Perrimon, N. (1994). Stripe-specific regulation of pair-rule genes by *hopscotch*, a putative Jak family tyrosine kinase in *Drosophila*. *Genes Dev* **8**, 300–312.

Blum, M. and Ott, T. (2018). Animal left–right asymmetry. *Curr Biol* **28**, R301–R304.

Brand, A. H. and Perrimon, N. (1993). Targeted gene expression as a means of altering cell fates and generating dominant phenotypes. *Development* **118**, 401–415.

Brown, S., Hu, N. and Hombría, J. C.-G. (2001). Identification of the first invertebrate interleukin JAK/STAT receptor, the *Drosophila* gene *domeless*. *Curr Biol* **11**, 1700–1705.

Calò, V., Migliavacca, M., Bazan, V., Macaluso, M., Buscemi, M., Gebbia, N. and Russo, A. (2003). STAT proteins: From normal control of cellular events to tumorigenesis. *J Cell Physiol* **197**, 157–168.

Cendrowski, J., Mamińska, A. and Miaczynska, M. (2016). Endocytic regulation of cytokine receptor signaling. *Cytokine Growth Factor Rev* **32**, 63–73.

Chang, E.-J., Ha, J., Kang, S.-S., Lee, Z. H. and Kim, H.-H. (2011). AWP1 binds to tumor necrosis factor receptor-associated factor 2 (TRAF2) and is involved in TRAF2-mediated nuclear factor-kappaB signaling. *Int J Biochem Cell Biol* **43**, 1612–1620.

Clague, M. J., Liu, H. and Urbé, S. (2012). Governance of Endocytic Trafficking and Signaling by Reversible Ubiquitylation. *Dev Cell* **23**, 457–467.

Coutelis, J., González-Morales, N., Géminard, C. and Noselli, S. (2014). Diversity and convergence in the mechanisms establishing L/R asymmetry in metazoa. *EMBO Rep* **15**, 926–937.

Devergne, O., Ghiglione, C. and Noselli, S. (2007). The endocytic control of JAK/STAT signalling in Drosophila. *J Cell Sci* **120**, 3457–3464.

Dong, B., Miao, G. and Hayashi, S. (2014). A fat body-derived apical extracellular matrix enzyme is transported to the tracheal lumen and is required for tube morphogenesis in *Drosophila*. *Development* **141**, 4104–4109.

Duan, W., Sun, B., Li, T. W., Tan, B. J., Lee, M. K. and Teo, T. S. (2000). Cloning and characterization of AWP1, a novel protein that associates with serine/threonine kinase PRK1 in vivo. *Gene* **256**, 113–121.

Elkin, S. R., Lakoduk, A. M. and Schmid, S. L. (2016). Endocytic pathways and endosomal trafficking: a primer. *Wien Med Wochenschr* **166**, 196–204.

Elliott, D. A. and Brand, A. H. (2008). The GAL4 system. In *Methods Mol Biol: Drosophila*, pp. 79–95. Humana Press.

Fenner, B. J., Scannell, M. and Prehn, J. H. M. (2009). Identification of polyubiquitin binding proteins involved in NF-κB signaling using protein arrays. *Biochim Biophys Acta* **1794**, 1010–1016.

Fleming, I. (1958). *Dr. No*. London: Jonathan Cape.

German, C. L., Sauer, B. M. and Howe, C. L. (2011). The STAT3 beacon: IL-6 recurrently activates STAT 3 from endosomal structures. *Exp Cell Res* **317**, 1955–1969.

Gesbert, F., Malardé, V. and Dautry-Varsat, A. (2005). Ubiquitination of the common cytokine receptor γc and regulation of expression by an ubiquitination/deubiquitination machinery. *Biochem Biophys Res Commun* **334**, 474–480.

Ghiglione, C., Devergne, O., Georgenthum, E., Carballès, F., Médioni, C., Cerezo, D. and Noselli, S. (2002). The *Drosophila* cytokine receptor Domeless controls border cell migration and epithelial polarization during oogenesis. *Development* **129**, 5437–5447.

Harrison, D. A., Binari, R., Nahreini, T. S., Gilman, M. and Perrimon, N. (1995). Activation of a *Drosophila* Janus kinase (JAK) causes hematopoietic neoplasia and developmental defects. *EMBO J* **14**, 2857–2865.

Harrison, D. A., McCoon, P. E., Binari, R., Gilman, M. and Perrimon, N. (1998). *Drosophila unpaired* encodes a secreted protein that activates the JAK signaling pathway. *Genes Dev* **12**, 3252–3263.

Hayashi, T. and Murakami, R. (2001). Left-right asymmetry in *Drosophila melanogaster* gut development. *Dev Growth Differ* **43**, 239–246.

Hayashi, S., Ito, K., Sado, Y., Taniguchi, M., Akimoto, A., Takeuchi, H., Aigaki, T., Matsuzaki, F., Nakagoshi, H., Tanimura, T., et al. (2002). GETDB, a database compiling expression patterns and molecular locations of a collection of Gal4 enhancer traps. *Genesis* **34**, 58–61.

Hayashi, M., Aono, H., Ishihara, J., Oshima, S., Yamamoto, H., Nakazato, Y. and Kobayashi, S. (2005). Left-right asymmetry in the alimentary canal of the *Drosophila* embryo. *Dev Growth Differ* **47**, 457–460.

Heyninck, K. and Beyaert, R. (1999). The cytokine-inducible zinc finger protein A20 inhibits IL-1-induced NF-κB activation at the level of TRAF6. *FEBS Lett* **442**, 147–150.

Hombría, J. C.-G., Brown, S., Häder, S. and Zeidler, M. P. (2005). Characterisation of Upd2, a Drosophila JAK/STAT pathway ligand. *Dev Biol* **288**, 420–433.

Hou, X. S., Melnick, M. B. and Perrimon, N. (1996). *marelle* Acts Downstream of the *Drosophila* HOP/JAK Kinase and Encodes a Protein Similar to the Mammalian STATs. *Cell* **84**, 411–419.

Hozumi, S., Maeda, R., Taniguchi, K., Kanai, M., Shirakabe, S., Sasamura, T., Spéder, P., Noselli, S., Aigaki, T., Murakami, R., et al. (2006). An unconventional myosin in *Drosophila* reverses the default handedness in visceral organs. *Nature* **440**, 798–802.

Hummel, T. and Klämbt, C. (2008). P-Element Mutagenesis. In *Methods Mol Biol: Drosophila*, pp. 97–117.

Inaki, M., Liu, J. and Matsuno, K. (2016). Cell chirality: its origin and roles in left-right asymmetric development. *Philos Trans R Soc Lond B Biol Sci* **371**, 20150403.

Inaki, M., Hatori, R., Nakazawa, N., Okumura, T., Ishibashi, T., Kikuta, J., Ishii, M., Matsuno, K. and Honda, H. (2018). Chiral cell sliding drives left-right asymmetric organ twisting. *Elife* **7**, e32506.

Jacque, E. and Ley, S. C. (2009). RNF11, a new piece in the A20 puzzle. *EMBO J* **28**, 455–456.

Jékely, G. and Rørth, P. (2003). Hrs mediates downregulation of multiple signalling receptors in *Drosophila*. *EMBO Rep* **4**, 1163–1168.

Jenett, A., Rubin, G. M., Ngo, T.-T., Shepherd, D., Murphy, C., Dionne, H., Pfeiffer, B. D., Cavallaro, A., Hall, D. and Jeter, J. (2012). A GAL4-driver line resource for Drosophila neurobiology. *Cell Rep* **2**, 991–1001.

Jiang, J., Kosman, D., Ip, Y. T. and Levine, M. (1991). The dorsal morphogen gradient regulates the mesoderm determinant twist in early Drosophila embryos. *Genes Dev* **5**, 1881–1891.

Katzmann, D. J., Babst, M. and Emr, S. D. (2001). Ubiquitin-Dependent Sorting into the Multivesicular Body Pathway Requires the Function of a Conserved Endosomal Protein Sorting Complex, ESCRT-I. *Cell* **106**, 145–155.

Kim, E. Y., Kim, J. E., Choi, B., Kweon, J., Park, S. O., Lee, H. S., Lee, E. J., Oh, S., Shin, H. R., Choi, H., et al. (2021). AWP1 Restrains the Aggressive Behavior of Breast Cancer Cells Induced by TNF-α. *Front Oncol* **11**, 1–11.

Kimelman, D. and Martin, B. L. (2012). Anterior-posterior patterning in early development: three strategies. *Wiley Interdiscip Rev Dev Biol* **1**, 253–266.

Kuroda, J., Nakamura, M., Yoshida, M., Yamamoto, H., Maeda, T., Taniguchi, K., Nakazawa, N., Hatori, R., Ishio, A., Ozaki, A., et al. (2012). Canonical Wnt signaling in the visceral muscle is required for left–right asymmetric development of the *Drosophila* midgut. *Mech Dev* **128**, 625–639.

Lee, J. H., Lee, C. W., Park, S. H. and Choe, K. M. (2017). Spatiotemporal regulation of cell fusion by JNK and JAK/STAT signaling during *Drosophila* wound healing. *J Cell Sci* **130**, 1917–1928.

Lei, J. T., Mazumdar, T. and Martinez-Moczygemba, M. (2011). Three lysine residues in the common β chain of the interleukin-5 receptor are required for janus kinase (JAK)-dependent receptor ubiquitination, endocytosis, and signaling. *J Biol Chem* **286**, 40091–40103.

Levin, M. (2005). Left–right asymmetry in embryonic development: a comprehensive review. *Mech Dev* **122**, 3–25.

Li, J., Li, W., Calhoun, H. C., Xia, F., Gao, F.-B. and Li, W. X. (2003). Patterns and functions of STAT activation during *Drosophila* embryogenesis. *Mech Dev* **120**, 1455–1468.

Lloyd, T. E., Atkinson, R., Wu, M. N., Zhou, Y., Pennetta, G. and Bellen, H. J. (2002). Hrs Regulates Endosome Membrane Invagination and Tyrosine Kinase Receptor Signaling in *Drosophila*. *Cell* **108**, 261–269.

Maeda, R., Hozumi, S., Taniguchi, K., Sasamura, T., Murakami, R. and Matsuno, K. (2007). Roles of single-minded in the left–right asymmetric development of the *Drosophila* embryonic gut. *Mech Dev* **124**, 204–217.

Martin-Bermudo, M. D., Dunin-Borkowski, O. M. and Brown, N. H. (1997). Specificity of PS integrin function during embryogenesis resides in the alpha subunit extracellular domain. *EMBO J* **16**, 4184–4193.

Martinez-Moczygemba, M., Huston, D. P. and Lei, J. T. (2007). JAK kinases control IL-5 receptor ubiquitination, degradation, and internalization. *J Leukoc Biol* **81**, 1137–1148.

Miyata, N., Okumoto, K., Mukai, S., Noguchi, M. and Fujiki, Y. (2012). AWP1/ZFAND6 Functions in Pex5 Export by Interacting with Cys-Monoubiquitinated Pex5 and Pex6 AAA ATPase. *Traffic* **13**, 168–183.

Moore, R., Vogt, K., Acosta-Martin, A. E., Shire, P., Zeidler, M. and Smythe, E. (2020). Integration of JAK/STAT receptor–ligand trafficking, signalling and gene expression in *Drosophila melanogaster* cells. *J Cell Sci* **133**, jcs246199.

Murthy, M., Garza, D., Scheller, R. H. and Schwarz, T. L. (2003). Mutations in the exocyst component Sec5 disrupt neuronal membrane traffic, but neurotransmitter release persists. *Neuron* **37**, 433–447.

Myllymäki, H. and Rämet, M. (2014). JAK/STAT Pathway in *Drosophila* Immunity. *Scand J Immunol* **79**, 377–385.

Naganathan, S. R., Middelkoop, T. C., Fürthauer, S. and Grill, S. W. (2016). Actomyosin-driven left-right asymmetry: From molecular torques to chiral self organization. *Curr Opin Cell Biol* **38**, 24–30.

Nakamura, M., Matsumoto, K., Iwamoto, Y., Muguruma, T., Nakazawa, N., Hatori, R., Taniguchi, K., Maeda, R. and Matsuno, K. (2013). Reduced cell number in the hindgut epithelium disrupts hindgut left–right asymmetry in a mutant of pebble, encoding a RhoGEF, in *Drosophila* embryos. *Mech Dev* **130**, 169–180.

Namigai, E. K. O., Kenny, N. J. and Shimeld, S. M. (2014). Right across the tree of life: The evolution of left-right asymmetry in the Bilateria. *Genesis* **52**, 458–470.

Okumura, T., Utsuno, H., Kuroda, J., Gittenberger, E., Asami, T. and Matsuno, K. (2008). The development and evolution of left-right asymmetry in invertebrates: Lessons from *Drosophila* and snails. *Dev Dyn* **237**, 3497–3515.

Okumura, T., Fujiwara, H., Taniguchi, K., Kuroda, J., Nakazawa, N., Nakamura, M., Hatori, R., Ishio, A., Maeda, R. and Matsuno, K. (2010). Left–right asymmetric morphogenesis of the anterior midgut depends on the activation of a non-muscle myosin II in *Drosophila*. *Dev Biol* **344**, 693–706.

Piper, R. C., Dikic, I. and Lukacs, G. L. (2014). Ubiquitin-dependent sorting in endocytosis. *Cold Spring Harb Perspect Biol* **6**, a016808.

Popichenko, D., Sellin, J., Bartkuhn, M. and Paululat, A. (2007). Hand is a direct target of the forkhead transcription factor Biniou during *Drosophila* visceral mesoderm differentiation. *BMC Dev Biol* **7**, 49.

Prudencio, P. and Guilgur, L. G. (2015). FLP/FRT Induction of Mitotic Recombination in *Drosophila* Germline. *Bio Protoc* **5**, e1458.

Recasens-Alvarez, C., Ferreira, A. and Milán, M. (2017). JAK/STAT controls organ size and fate specification by regulating morphogen production and signalling. *Nat Commun* **8**, 13815.

Ren, W., Zhang, Y., Li, M., Wu, L., Wang, G., Baeg, G.-H., You, J., Li, Z. and Lin, X. (2015). Windpipe Controls *Drosophila* Intestinal Homeostasis by Regulating JAK/STAT Pathway via Promoting Receptor Endocytosis and Lysosomal Degradation. *PLoS Genet* **11**, e1005180.

Rothe, M., Sarma, V., Dixit, V. and Goeddel, D. (1995). TRAF2-Mediated Activation of NF-KB by TNF Receptor 2 and CD40. *Science (1979)* **267**, 1494–1498.

Seif, F., Khoshmirsafa, M., Aazami, H., Mohsenzadegan, M., Sedighi, G. and Bahar, M. (2017). The role of JAK-STAT signaling pathway and its regulators in the fate of T helper cells. *Cell Commun Signal* **15**, 23.

Seo, J.-H., Park, D.-S., Hong, M., Chang, E.-J. and Choi, S.-C. (2013). Essential role of AWP1 in neural crest specification in *Xenopus*. *Int J Dev Biol* **57**, 829–836.

Shimizu, H., Woodcock, S. A., Wilkin, M. B., Trubenová, B., Monk, N. A. M. and Baron, M. (2014). Compensatory Flux Changes within an Endocytic Trafficking Network Maintain Thermal Robustness of Notch Signaling. *Cell* **157**, 1160–1174.

Shin, D., Nakamura, M., Morishita, Y., Eiraku, M., Yamakawa, T., Sasamura, T., Akiyama, M., Inaki, M. and Matsuno, K. (2021). Collective nuclear behavior shapes bilateral nuclear symmetry for subsequent left-right asymmetric morphogenesis in *Drosophila*. *Development* **148**, dev198507.

Song, H. Y., Rothe, M. and Goeddel, D. v. (1996). The tumor necrosis factor-inducible zinc finger protein A20 interacts with TRAF1/TRAF2 and inhibits NF-κB activation. *PNAS* **93**, 6721–6725.

Spéder, P., Ádám, G. and Noselli, S. (2006). Type ID unconventional myosin controls left-right asymmetry in *Drosophila*. *Nature* **440**, 803–807.

Spradling, A. and Rubin, G. (1982). Genetic Transformation of *Drosophila* with Transposable Element Vectors. *Science (1979)* **218**, 341–347.

Stapleton, M., Liao, G., Brokstein, P., Hong, L., Carninci, P., Shiraki, T., Hayashizaki, Y., Champe, M., Pacleb, J., Wan, K., et al. (2002). The *Drosophila* gene collection: identification of putative full-length cDNAs for 70% of *D. melanogaster* genes. *Genome Res* **12**, 1294–1300.

Tanaka, T. and Nakamura, A. (2008). The endocytic pathway acts downstream of Oskar in *Drosophila* germ plasm assembly. *Development* **129**, 517.

Taniguchi, K., Hozumi, S., Maeda, R., Ooike, M., Sasamura, T., Aigaki, T. and Matsuno, K. (2007). D-JNK signaling in visceral muscle cells controls the laterality of the *Drosophila* gut. *Dev Biol* **311**, 251–263.

Thurmond, J., Goodman, J. L., Strelets, V. B., Attrill, H., Gramates, L. S., Marygold, S. J., Matthews, B. B., Millburn, G., Antonazzo, G., Trovisco, V., et al. (2019). FlyBase 2.0: the next generation. *Nucleic Acids Res* **47**, D759–D765.

Toba, G., Ohsako, T., Miyata, N., Ohtsuka, T., Seong, K.-H. and Aigaki, T. (1998). The Gene Search System: A Method for Efficient Detection and Rapid Molecular Identification of Genes in *Drosophila melanogaster*. *Genetics* **133**, 347–359.

Tognon, E., Wollscheid, N., Cortese, K., Tacchetti, C. and Vaccari, T. (2014). ESCRT-0 Is Not Required for Ectopic Notch Activation and Tumor Suppression in *Drosophila*. *PLoS One* **9**, e93987.

Tsurumi, A., Xia, F., Li, J., Larson, K., LaFrance, R. and Li, W. X. (2011). STAT Is an Essential Activator of the Zygotic Genome in the Early Drosophila Embryo. *PLoS Genet* **7**, e1002086.

Utsunomiya, S., Sakamura, S., Sasamura, T., Ishibashi, T., Maeda, C., Inaki, M. and Matsuno, K. (2019). Cells with Broken Left–Right Symmetry: Roles of Intrinsic Cell Chirality in Left–Right Asymmetric Epithelial Morphogenesis. *Symmetry (Basel)* **11**, 505.

Vandenberg, L. N. and Levin, M. (2013). A unified model for left–right asymmetry? Comparison and synthesis of molecular models of embryonic laterality. *Dev Biol* **379**, 1–15.

Vidal, O. M., Stec, W., Bausek, N., Smythe, E. and Zeidler, M. P. (2010). Negative regulation of *Drosophila* JAK-STAT signalling by endocytic trafficking. *J Cell Sci* **123**, 3457–3466.

Wodarz, A., Hinz, U., Engelbert, M. and Knust, E. (1995). Expression of *crumbs* confers apical character on plasma membrane domains of ectodermal epithelia of *Drosophila*. *Cell* **82**, 67–76.

Wölfler, A., Irandoust, M., Meenhuis, A., Gits, J., Roovers, O. and Touw, I. P. (2009). Site-specific ubiquitination determines lysosomal sorting and signal attenuation of the granulocyte colony-stimulating factor receptor. *Traffic* **10**, 1168–1179.

Yan, R., Small, S., Desplan, C., Dearolf, C. R. and Darnell, J. E. (1996). Identification of a *Stat* Gene That Functions in *Drosophila* Development. *Cell* **84**, 421–430.

Yao, K.-M. and White, K. (1994). Neural Specificity of *elav* Expression: Defining a *Drosophila* Promoter for Directing Expression to the Nervous System. *J Neurochem* **63**, 41–51.

Yoshiba, S. and Hamada, H. (2014). Roles of cilia, fluid flow, and Ca^{2+} signaling in breaking of left-right symmetry. *Trends Genet* **30**, 10–17.

ACKNOWLEDGMENTS

I would like to express my sincere gratitude to my advisor Dr. Kenji Matsuno for his continued encouragement and guidance throughout this study.

I would also like to express my appreciation for my committee members, Dr. Hiroki Nishida and Dr. Hiroki Oda, for their thoughtful inputs and critical advice.

Special thanks are given to previous graduate students, staffs and collaborators: Takeshi Sasamura*, Mikiko Inaki*, Junpei Kuroda, Reo Maeda, Ryo Hatori, Tomoki Ishibashi, Kiichiro Taniguchi, Masashi Ooike, Tomohiro Taguchi, Naotaka Nakazawa, Mitsutoshi Nakamura, Shunya Hozumi, Takashi Okumura, Toshiro Aigaki that have contributed to this research. (The first two people marked with * contributed the most to this project.)

I also thank the current and previous members of the Matsuno laboratory for their critical inputs for my thesis and continued help and support throughout this study.

Much gratitude is also given to the research groups (Dr. Norbert Perrimon, Dr. Stephane Noselli, Dr. Hugo Bellen, and Dr. Akira Nakamura) and stock centers (*Drosophila* Genetic Resource Center, Bloomington *Drosophila* Stock Center, and Developmental Studies Hybridoma Bank) that provided some of the fly lines and antibodies used in this study.

Finally, I express deep appreciation for my family and friends who have provided immense motivation, support and encouragement throughout this study.

This work was supported by the Japan Society for the Promotion of Science KAKENHI.